



# *Reigitherium* (Meridiolestida, Mesungulatoidea) an Enigmatic Late Cretaceous Mammal from Patagonia, Argentina: Morphology, Affinities, and Dental Evolution

Tony Harper<sup>1</sup> · Ana Parras<sup>2</sup> · Guillermo W. Rougier<sup>3</sup>

Published online: 4 May 2018

© Springer Science+Business Media, LLC, part of Springer Nature 2018

## Abstract

New dental and dentary fossils collected in the Upper Cretaceous La Colonia Formation in central Patagonia provide new evidence on the morphology, feeding ecology, and relationships of the enigmatic mammal *Reigitherium*. The newly discovered specimens described here include elements of the upper dentition and several partial dentaries, elucidating fundamental questions of serial homology and postcanine dental formula (four premolars and three molars). This new evidence supports a nested position of *Reigitherium* within the advanced meridiolestidan clade Mesungulatoidea. Apomorphic features of the upper and lower molariform elements include intense enamel crenulation circumscribed within the primary trigon and trigonid, elevated cingulids, and the neomorphic appearance of cusps/cuspidulids, all of which increase overall crown complexity. A Dental Topography Analysis comparing *Reigitherium* and its sister taxon *Peligrotherium* to Cretaceous and Cenozoic therians demonstrates functional similarity between the mesungulatoids and South American marsupial taxa that succeed them in the small-to-medium-sized herbivore niche during the Paleocene. Previous taxonomic attributions of *Reigitherium* are discussed and comparisons with other meridiolestidans highlight the remarkable radiation of this group in the Cretaceous of South America.

**Keywords** *Reigitherium* · Meridiolestida · Dental complexity · Mesozoic Mammalia

## Introduction

Concurrent with the initial division and differentiation of the Late Cretaceous lineages of the crown group Theria in the Northern Hemisphere (Archibald and Deutschman 2001; Grossnickle and Polly 2013; Halliday and Goswami 2016; Grossnickle and Newham 2016), the mammalian fauna of South America had already achieved a state of prominent

diversity within microvertebrate fossil assemblages (Rougier et al. 2010). The most abundant and diverse of these Late Cretaceous Gondwanan endemic mammals are referable to a monophyletic grouping of stem therians termed the Meridiolestida (Rougier et al. 2011). These species therefore represent an independent phylogenetic experiment with which to compare the trajectory of mammalian evolution in northern continents before and near the K-Pg boundary (e.g., Jernvall et al. 1996; Woodburne et al. 2014).

Morphological comparisons using meridiolestidans are also particularly valuable because of the specific craniodental similarities between meridiolestidans and hypothetical reconstructions of the therian common ancestor, such as the reduction to three molars and an enlarged and triangular fifth-from-last successor tooth (blade-like in early therians, but pyramidal in the Meridiolestida; McKenna 1975; Prothero 1981; Luckett 1993; Rougier et al. 2012). Because of their likely derivation from Jurassic dryolestoids (or a related pretribosphenic group with similar dental formulae and crown morphology), many of these similarities are likely the result of convergence and/or parallelism, in addition to shared ancestry (Gould 2002). These features, combined with the retention of stem therian

**Electronic supplementary material** The online version of this article (<https://doi.org/10.1007/s10914-018-9437-x>) contains supplementary material, which is available to authorized users.

✉ Guillermo W. Rougier  
grougier@louisville.edu

<sup>1</sup> Center for Functional Anatomy and Evolution, Johns Hopkins University, 1830 E. Monument St, Baltimore, MD 21205, USA

<sup>2</sup> INCITAP (CONICET-UNLPam), Facultad de Ciencias Exactas y Naturales, Universidad Nacional de La Pampa, Uruguay 151, 6300 Santa Rosa, La Pampa, Argentina

<sup>3</sup> Department of Anatomical Sciences and Neurobiology, University of Louisville, 511 S. Floyd St, Louisville, KY 40202, USA

symplesiomorphies, have also underwritten much of the confusion seen in the taxonomic history of the better known meridiolestidan taxa. For example, the fossorial *Necrolestes* (Rougier et al. 2012; Wible and Rougier 2017) has been variously interpreted as an aberrant metatherian or eutherian, and the large herbivorous *Peligrotherium* (Bonaparte et al. 1993; Gelfo and Pascual 2001) was first assigned to the eutherian family Peritychidae.

The latest Cretaceous meridiolestidan *Reigitherium* (Figs. 1 and 2) has been the subject of an altogether different battery of alternative interpretations. While originally described as a dryolestoid by Bonaparte (1990), several later authors ascribed it to a stem mammaliaform group far distant from the crown clade Theria (Pascual et al. 2000). This diversity of opinion has been enabled by the limited material and highly derived morphology presented by this taxon, which has been commented on by Kielan-Jaworowska et al. (2004) as warranting an ordinal distinction from Docodonta. These authors subsequently assigned *Reigitherium* to Mammalia (*sensu lato*), subclass and order incertae sedis.

Additionally, while being distinctive at the generic level, the ornamented and labially distended morphology seen in the molariforms of *Reigitherium* has made diagnosis of the principal anatomical axes (mesiodistal, labiolingual, etc.) and the upper versus lower attribution of isolated dental elements uniquely problematic. The apomorphic complexity and

ambiguity manifest in the dentition of *Reigitherium* have caused the misidentification of its holotype, a lower right molar recovered from the Los Alamitos Formation (described as an upper left molariform in its initial description by Bonaparte 1990). The later report of three sequential lower postcanines (p3, p4, and m1 based on current interpretations) preserved in situ by a dentary fragment recovered from the La Colonia Formation made clear the lower molar identity of the type specimen (Pascual et al. 2000). However, based on this evidence these authors transferred *Reigitherium* (within a monotypic family) from Dryolestoidea to Docodonta, a clade currently unrecorded from South America (however, see Martin et al. 2013).

Expanded samples of isolated dental and gnathic remains recovered from two localities in the La Colonia Formation during field expeditions organized by one of us (GWR) in collaboration with the Museo Paleontológico Egidio Feruglio (MPEF) corroborate the original taxonomic assignment of *Reigitherium* as a dryolestoid (or dryolestoid-like) mammal, and further underscore its eccentric position outside the range of dental morphologies known in any other stem therian lineage (Patterson 1956; Hershkovitz 1971; Kielan-Jaworowska et al. 2004). These new and better preserved specimens also greatly clarify major aspects of cusp homology, dental formula, and the phylogenetic placement of *Reigitherium* among the advanced meridiolestidans. This

**Fig. 1** Reconstruction of upper postcanine series. Schematic illustrations of upper left penultimate and ultimate premolars and molars in **a** *Peligrotherium*; **b** *Coloniatherium*; and **c** *Reigitherium*

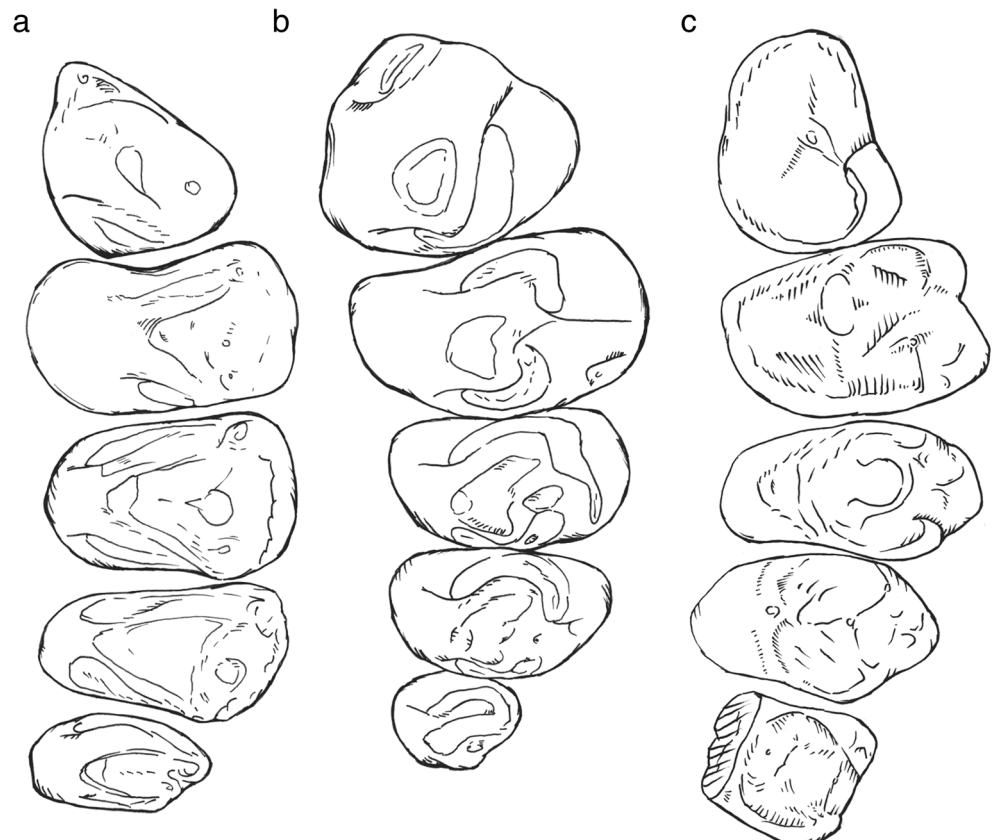
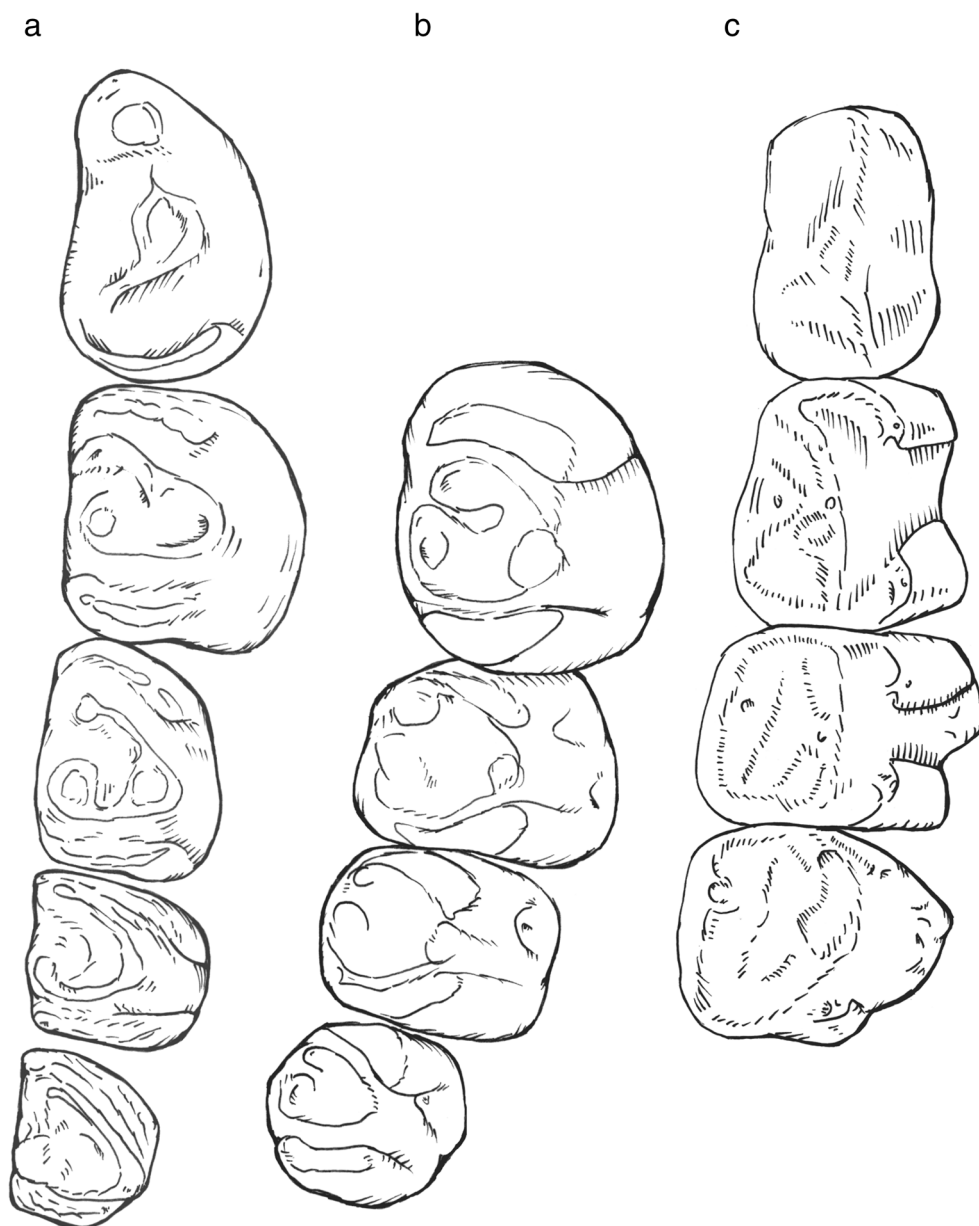


**Fig. 2** Reconstruction of lower postcanine series. Schematic illustrations of lower right penultimate and ultimate premolars and molars in **a** *Peligrotherium*; **b** *Coloniatherium*; and **c** *Reigitherium*



report summarizes the provenance and anatomy of these new specimens, and provides explicit comparisons with the dentition of better known meridiolestidans and other crown mammals.

**Study Area and Sample Provenance** The new specimens come from middle strata of the La Colonia Formation (second facies association of Pascual et al. 2000), in the “Anfiteatro” area, located at the southeastern slope of the Sierra de La Colonia, in the vicinity of Cerro Bayo, Chubut Province (Argentina). The exposed sedimentary rocks in this area are characterized by the predominance of massive or laminated claystones and siltstones, with intercalations of massive, laminated or cross-bedded sandstones (see “Norte de Cerro Bayo 1” and “Norte de Cerro Bayo 2” sections, in Gasparini et al. 2015).

Mammal remains were collected from intercalated, very thin lenses (< 0.2 m) of scarce lateral extension, located ~70 m from the bottom of the outcrops as part of a column sampling in search of microfossils. The lenses have a pelitic-sandy matrix with abundant gypsum, and consist of millimeter-scale remains of aquatic and terrestrial vertebrates, mainly fishes, but also and in very low proportion mammals, amphibians, and reptiles. The specimens are mostly concentrated in a bed of ~1 to 4 cm in thickness, are disarticulated and chaotically oriented, and most of them are fragmented with rounded and polished broken surfaces showing a high degree of alteration. The fossils are poorly sorted by size, with complete isolated elements smaller than a millimeter preserved together with relatively large isolated dinosaur bones (several tens of centimeters). The taphonomic attributes suggest that

the fossil producing layers were formed by hydraulic transport of the fossils previous to their deposition (Varela and Parras 2013; Gasparini et al. 2015). The unsorted composition and thin vertical extent of these lenses suggest that their genesis is attributable to discrete sedimentary events (such as storm surges or mass wasting) in which current velocity rapidly drops to zero. The new specimens described here come from two separate localities El Uruguayo (Rougier et al 2009b) and Anfiteatro 1 (coordinates available upon request).

**Geological Background** The La Colonia Formation (Pesce 1979) crops out along the south-eastern margin of the Somún Curá Plateau, northern central Chubut Province, Argentina. This stratigraphic unit represents a variety of paleoenvironments including fluvial, marginal marine, and shallow marine deposits (Ardolino and Franchi 1996; Pascual et al. 2000), originating during the initial stages of the Late Cretaceous/Paleocene transgression from the Atlantic Ocean in Patagonia.

At the Sierra de La Colonia area, three facies associations were described as occurring in the La Colonia Formation (Pascual et al. 2000). According to these authors the lowermost facies association is characterized by cross-bedded sandstones and conglomerates deposited in a moderate to low sinuosity fluvial environment. However, Cúneo et al. (2014) interpreted these deposits as representing shoreface sedimentation dominated by bi-modal processes, a product of the initial phase of the Late Cretaceous Atlantic transgression.

The second facies association is the thickest and most representative of the La Colonia Formation and contains most of the vertebrate remains, and aquatic and terrestrial plants, so far collected (e.g., Pascual et al. 2000; Rougier et al. 2009b; O’Gorman et al. 2013; Cúneo et al. 2014; Gasparini et al. 2015). It is composed mostly of massive and laminated claystone-siltstone with intercalations of massive, laminated, or cross-bedded sandstones deposited in marginal marine environments, such as estuaries, tidal flats, littoral lagoons, or coastal plains, influenced by both freshwater stream flows from the continent and tidal currents from the sea (Ardolino and Delpino 1987; Page et al. 1999; Pascual et al. 2000; Gasparini et al. 2015). From sedimentological characteristics together with ecological requirements of the well-preserved collected fauna (mostly terrestrial, fresh, and brackish water taxa), Gasparini et al. (2015) suggested that deposition would have been mostly in low-energy restricted environments, like muddy flood plains, marshes, and ponds cut by meandering channels, probably in the central mixed-energy zone within an estuary. Alternatively, sedimentary deposits outcropping between Cerro Bosta locality and the Cañadón del Irupé/Quebrada del Helecho were interpreted by Cúneo et al. (2014) as a barrier-island/lagoon complex occurring along irregular clastic coastal plains bathed by shallow seas.

The uppermost facies association is composed of laminated claystones containing remains of bivalves and it was regarded as deposited in the upper part of an intertidal flat environment (Pascual et al. 2000). Toward the northeast in the Telsen area, Guler et al. (2014) recognized, based on the composition of palynological assemblages and sedimentological data, a progressive upward-shallowing trend for this upper part of the La Colonia Formation, consisting of shoreface to offshore deposits at the bottom and intertidal-flat to supratidal environments toward the top.

Regarding the age of the La Colonia Formation, at the study area the base is marked by the unconformity that separates this unit from the subjacent rocks of the Cerro Barcino Formation of the Chubut Group. Geochronological data from the uppermost part of the Cerro Barcino Formation in the margins of the Río Chubut, south of the study area, gave a U-Pb zircon age of ~97.4 Ma, constraining the Chubut Group to an age not younger than the Cenomanian (Suárez et al. 2014). Therefore, the age of the base of the La Colonia Formation depends on the time span encompassed by the unconformity below, but could not be older than Cenomanian. On the other hand, Ardolino and Franchi (1996), based on micropaleontological data, regarded the upper part of this unit as Campanian-Maastrichtian in age. Recently, Guler et al. (2014), based on palynological data, suggested an age not older than Paleocene for the uppermost part of the unit in the Telsen area. In short, the La Colonia Formation was deposited in the Late Cretaceous, most probably during the Campanian–Maastrichtian, with the uppermost strata extending to the Paleocene. The Late Cretaceous Los Alamitos Formation is also interpreted as being of Campanian–Maastrichtian age and yielded the type specimen of *Reigitherium bunodontum*, an isolated molar (Bonaparte 1990; see below). The facies yielding mammals in the Los Alamitos Formation reflects shallow lacustrine to lagoonal environments with a likely near-shore location and laterally interdigitating with marine sediments (Andreis 1987; Andreis et al. 1989). Both the La Colonia and Los Alamitos formations were deposited as part of the epeiric sea environment formed by the fragmented archipelago developed in what is present-day northern Patagonia during the Late Cretaceous–Paleocene Atlantic transgression (Malumián and Caramés 1995; Goin et al. 2016) and the invasion of the extensive Kawas sea (Riccardi 1987; Hugo and Leanza 2001). Based on faunal composition it is likely, but not certain, that the specimens from La Colonia Formation are younger than those from both the Los Alamitos Formation and the contemporaneous (or near contemporaneous) Allen Formation in northernmost Patagonia (Rougier et al. 2009a).

## Materials and Methods

A few isolated mammalian teeth were found by one of us (AP) during the processing of sediment samples in search of



microfossils. The sediment was soaked and washed in a screen with a 6.2 mm aperture that removed the bulk of the pelitic fraction and then separated in fractions using screens with 4, 2, and 1 mm of mesh size. The picking was done manually under binocular microscope and mammalian specimens were recovered from all fractions. Variations of this procedure were used more recently (GWR and collaborators) to process larger samples aimed at microvertebrate collection, such as using a deflocculant: sodium silicate ( $\text{Na}_2\text{SiO}_3$ ) with a 1.4–7 specific density, which was very helpful to shorten the pre-wash soaking of the sediment. The final mesh size was reduced to 0.65 mm.

Systematic analyses including *Reigitherium* and nine other taxa referable to Mesungulatoidea, Meridiolestida, and/or Dryolestoidea were conducted using phylogenetic estimations based on both Maximum Parsimony and Bayesian (maximum a posteriori) optimality criteria. These tree searches were implemented with the programs PAUP\* version 4.0 (Swofford 2002) and MrBayes version 3.2 (Ronquist et al. 2012) using standard parameterizations, as described below. Convergence diagnostics were checked for the Bayesian analysis using programs packaged with the program BEAST (Drummond and Bouckaert 2015).

Quantification of high-level morphological features in the lower second molars from a comparative sample of tribosphenic mammals, *Reigitherium*, and *Peligrotherium* are reported below in the context of a Dental Topography Analysis (Evans et al. 2007; Boyer 2008; Bunn et al. 2011). Dental metrics were measured from surface files generated from surface scans and CT imaging. Because all surface information is subsampled to approximately 10,000 triangular faces before further processing, no systematic difference in topography is detectable between data generated from either method. The Bissekty eutherians were micro-CT scanned at 27  $\mu\text{m}$  resolution using the GE Explore Locus rodent CT scanner housed at the Moores Cancer Institute at the University of California, San Diego. The marsupial taxa and *Peligrotherium* were scanned using a HDI Advance white light surface scanner. Finally, the specimen of *Reigitherium* used was converted to a surface file from approximately 9- $\mu\text{m}$  resolution micro-CT images generated at the Shared Materials Instrumentation Facility (SMIF) at Duke University. All surface files were cropped and edited using default smoothing and re-meshing algorithms implemented by the programs Amira and Geomagic Wrap. All surface editing protocols followed guidelines recommended by Spradley et al. (2017); and computations were performed with the R package *Molar* (Pampush et al. 2016). The anatomical terminology employed for the following descriptions follows Kielan-Jaworowska et al. (2004) and Rougier et al. (2009a, 2011, 2012) unless otherwise indicated (Fig. 3).

All data generated or analyzed for this study are included in the supplementary materials associated with this publication,

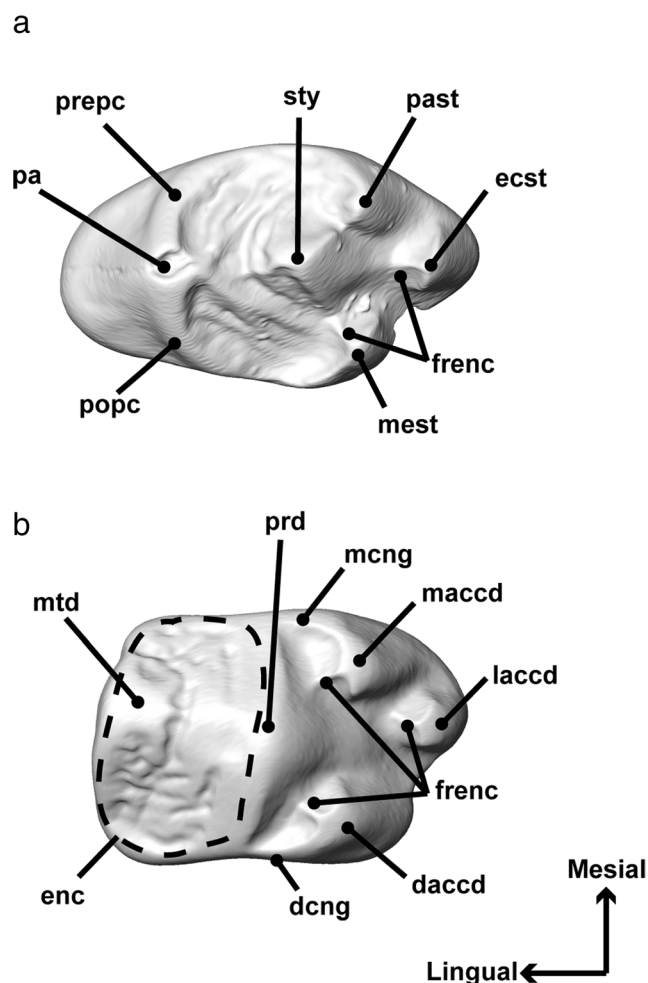


**Fig. 3** Crown terminology used here. **a** upper molariform features: ecst, ectostyle (accessory cusp); frenc, frenular crests; mest, metastyle; pa, paracone; past, parastyle; popc, postparacrista; prepc, preparacrista; sty, stylocone. **b** lower molariform features: daccd, distal accessory cuspid; dcng, distal cingulid; enc, enceinte; frenc, frenular crests; laccd, labial accessory cuspid; maccd, mesial accessory cuspid; mcng, mesial cingulid; mtd, metaconid; prd, protoconid

in addition to a table summarizing all new specimens of *Reigitherium* described below. Surface files of all lower second molars included in our Dental Topographic Analysis, and several additional surface models of *Reigitherium*, are available from the corresponding author upon request.

**Institutional Abbreviations** CCMGE, Cheryshev’s Central Museum of Geological Exploration, St. Petersburg, Russia; FMNH, Field Museum of Natural History, Chicago; MACN, Museo Argentino de Ciencias Naturales “Bernardino Rivadavia,” Buenos Aires, Argentina; MLP, Museo de La Plata, La Plata, Argentina; MNHN, Institut de Paléontologie, Muséum National d’Histoire Naturelle, Paris, France; MNRJ, Museo Nacional Rio de Janeiro, Rio de Janeiro, Brazil; MPEF-PV, Museo Paleontológico Egidio Feruglio, Chubut, Argentina, Paleontología de Vertebrados;

URBAC, Uzbek/Russian/British/American/Canadian joint paleontological expedition specimens; ZIN, Zoological Institute of the Russian Academy of Sciences, St. Petersburg, Russia.

## Systematic Paleontology

Class MAMMALIA Linnaeus, 1758  
 Clade CLADOTHERIA McKenna, 1975  
 Superorder DRYOLESTOIDEA Butler, 1939  
 Order MERIDIOLESTIDA Rougier et al., 2011  
 Clade MESUNGULATOIDEA Rougier et al., 2011  
 Family REIGITHERIIDAE Bonaparte, 1990

*Reigitherium* Bonaparte, 1990

**Type Species** *Reigitherium bunodontum* Bonaparte, 1990. The specific epithet was changed from *bunodonta* to *bunodontum* by Pascual et al. (2000), to match the neutral gender of the genus.

**Holotype** MACN-RN-173: An isolated and fragmentary lower right m2, recovered from the “green-colored bed just below the concretionary top of the Cerrito del Mamífero, middle section of the Los Alamitos Formation” (Bonaparte 1990: 66). West Slope of Cerro Cuadrado locality, Arroyo Verde, Río Negro province, Patagonia, Argentina.

**Distribution** Latest Cretaceous (Campanian-Maastrichtian); “Alamitan” South American Land Mammal Age (SALMA). Los Alamitos and La Colonia formations. Río Negro and Chubut provinces, Argentina.

**Referred Specimens** MPEF-PV 606: A partial left dentary preserving lower premolars 3–4 and the lower first molar, described by Pascual et al. (2000). Recovered from the “second facies association of the La Colonia Formation, on the southern slopes of the North Patagonian Massif” (Pascual et al. 2000: 402), Chubut province, Patagonia, Argentina.

The new specimens described below were recovered from the El Uruguayo and Anfiteatro 1 localities, upper part of the La Colonia Formation, Chubut province, Patagonia, Argentina. These specimens include: MPEF-PV 2014, dentary fragment; MPEF-PV 2020, dentary fragment; MPEF-PV 2072, P4; MPEF-PV 2237, m2; MPEF-PV 2238, M1; MPEF-PV 2317 m1; MPEF-PV 2339, P3; MPEF-PV 2341, M2; MPEF-PV 2343, upper molar; MPEF-PV 2344, P4; and MPEF-PV 2337, dentary fragment; MPEF-PV 2338, dentary fragment; MPEF-PV 2347, c1; MPEF-PV 2349, C1; MPEF-PV 2368, p1; MPEF-PV 2369, M3; MPEF-PV 2372, dentary fragment; MPEF-PV 2373, P4; MPEF-PV 2375, C1; MPEF-PV 2376, p3; respectively. A

complete listing of the new La Colonia specimens described here is available in the online supplementary materials associated with this report (Online Resource 1).

**Diagnosis** A very small mesungulatoid with simple premolars increasing in size posteriorly to an enlarged molariform fourth premolar; and three complex and mediolaterally extended molars decreasing in size posteriorly. Compared to the better known mesungulatoids *Coloniatherium* (Rougier et al. 2009b) and *Peligrotherium* (Paez-Arango 2008), *Reigitherium* is much smaller and shows the presence of several autapomorphic dental specializations: 1) interradicular crests (McDowell 1958) connecting the roots of upper and lower canine and postcanine elements, 2) highly crenulated trigonids and primary trigons, with an enclosing encainte structure in the lower molars, and 3) neomorphic ectostyles on the upper first and second molars, and neomorphic accessory cusplids (also seen in *Peligrotherium*) distributed within the labial portion of the lower molariforms.

## Descriptions

The environment of deposition and method of discovery have had significant effects on the state of preservation of the fossils described here. Because of the postmortem hydraulic transport of the La Colonia Formation fossils, there has been moderate to extensive rounding of most specimens. Additionally, the bulk sampling and screen washing procedures used to recover and concentrate these specimens may have caused some additional fracturing of the gnathic specimens in particular. The imprint of postmortem wear does obscure many details of texture, use-wear, and unworn morphology in the dental and dentary remains described below; however, it is improbable that the fracturing and rounding produced by these processes will be mistaken for premortem morphology. Additionally, several of the better preserved dental specimens show no significant postmortem damage. In particular, the newly discovered locality Anfiteatro 1 bears a relative abundance of well-preserved mammalian jaws, which, when combined with previously recovered specimens (Pascual et al. 2000; Rougier et al. 2009b), have proved crucial in the determination of dental formula.

**Dentary** Features of the mandibular corpus and base of the ascending ramus can be seen in the specimens, MPEF-PV 2014, MPEF-PV 2337, MPEF-PV 2338, and MPEF-PV 2372 (Figs. 4, 5, 6 and 7). All of these are fragmentary dentaries, missing the anterior most and posterior most structures of the lower jaw. The MPEF-PV 2337 (Fig. 5) specimen is the most completely preserved and provides the bulk of anatomical detail described below.

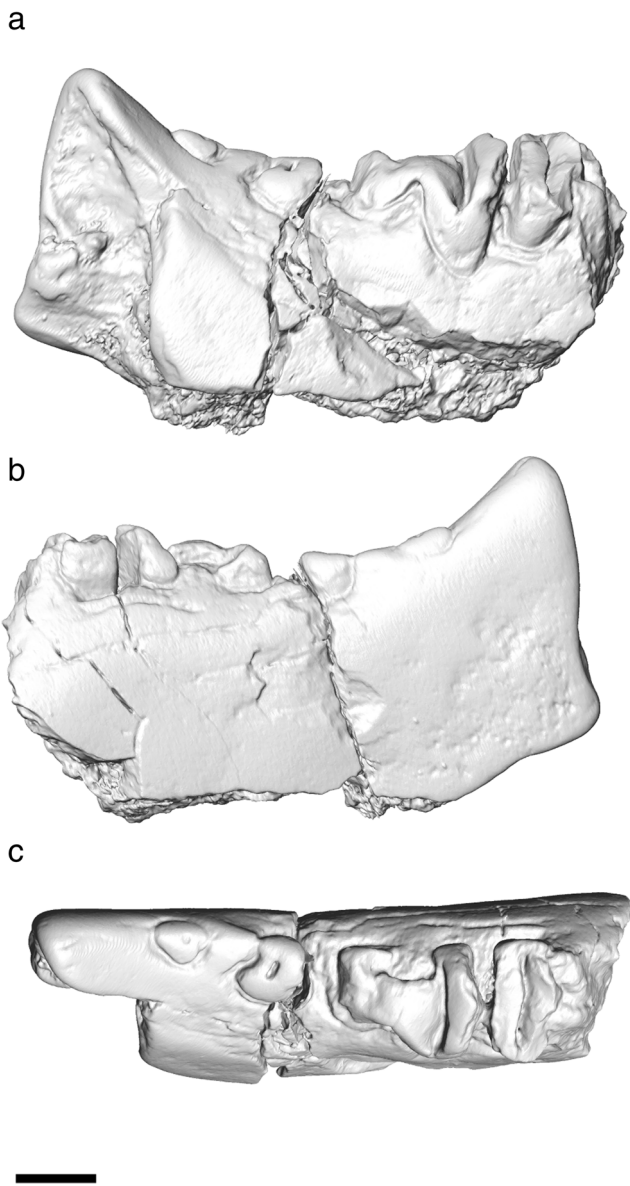


**Fig. 4** *Reigitherium* MPEF-PV 1214. Posterior left dentary fragment (reversed) showing molar alveoli and associated roots. **a** labial view; **b** lingual view; **c** occlusal view. Scale bar is 1 mm

The ventral contour of the mandibular corpus is semicircular inferior to the postcanine tooth row and continues posteriorly to form a point of inflection inferior to the base of the ascending ramus, termed the angular notch. An angular process is known to be present in the better known meridiolestidan taxa *Cronopio* and *Peligrotherium* (Paez-Arango 2008; Rougier et al. 2011), and in an unassigned mesungulatoid dentary described by Forasiepi et al. (2012). This phylogenetic bracket, combined with the presence of an angular notch in *Reigitherium*, suggests the presence of an angular process in this species as well.

The anterior region of the ascending ramus shows the base of the coronoid process sloping posteriorly at an angle of

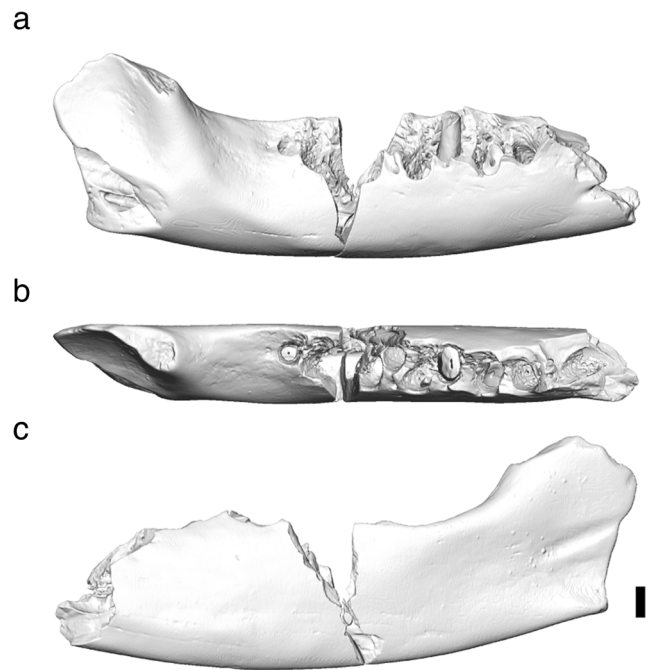


**Fig. 5** *Reigitherium* MPEF-PV 2337. Fragmentary left dentary bone (reversed). **a** labial view; **b** occlusal view; **c** lingual view. Scale bar is 1 mm

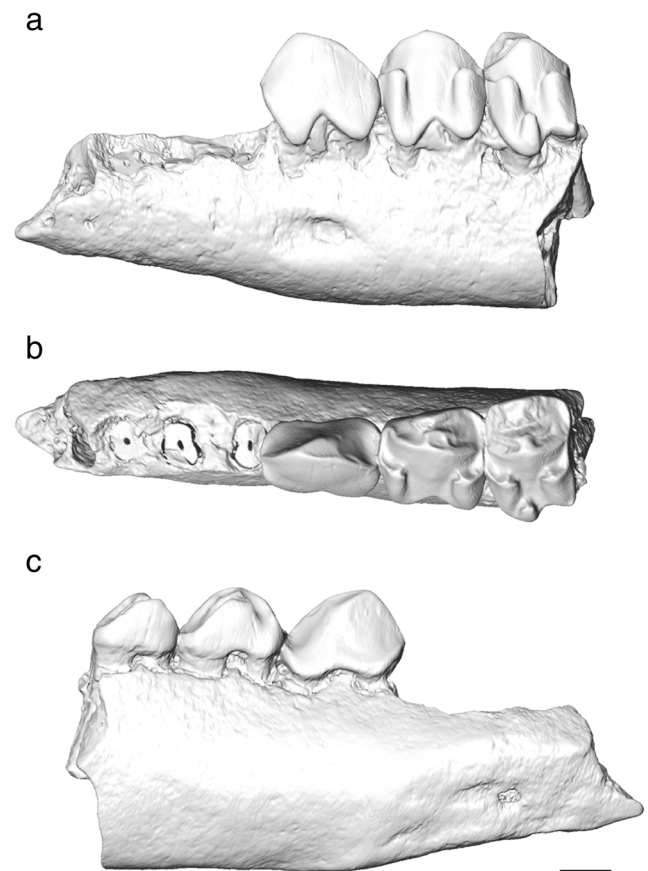


**Fig. 6** *Reigitherium* MPEF-PV 2338. Fragmentary right dentary bone (reversed) with p3, p4, and m1. **a** labial view; **b** occlusal view; **c** lingual view. Scale bar is 1 mm



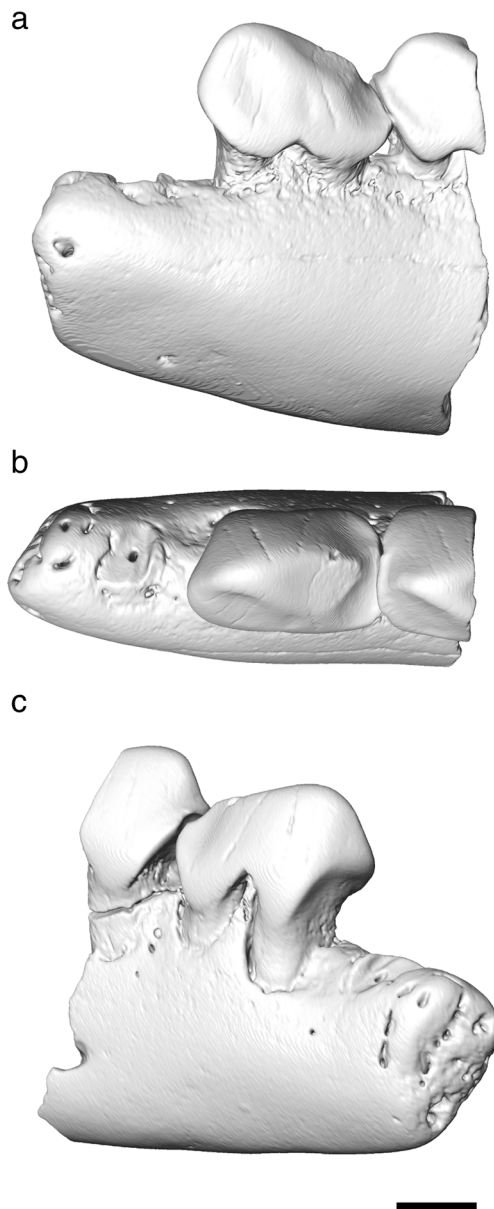


**Fig. 7** *Reigitherium* MPEF-PV 2372. Fragmentary left dentary bone (reversed) with p2 and mesial half of p3. **a** lingual view; **b** occlusal view; **c** anterolabial view. Scale bar is 1 mm

approximately 45 degrees. The anterior border of the coronoid process is smoothly convex in a horizontal plane, and lacks evidence of an appositional contact with a coronoid bone. The region of bone directly lateral to the base of the coronoid process is damaged in all available specimens, and what is probably the rostral margin of the masseteric fossa on the lateral aspect of the coronoid process is obscured. The medial side of the base of the coronoid process and ascending ramus is undamaged and is smoothly flattened in a parasagittal plane, displaying the absence of an anteriorly placed mandibular foramen, Meckel's sulcus, or anteriorly extended pterygoid flange. The lingual surface of the mandibular corpus is also smoothly convex under the tooth row.

The specimens MPEF-PV 2338 and MPEF-PV 2372 (Figs. 6–7) preserve the outline of the mandibular symphysis; however, in both cases its morphology has been partially effaced by postmortem abrasion and fracturing of the anterior dentary. It can still be determined that the symphysis was neither fused nor highly interdigitating, and that it took the form of a horizontally extended oval in medial view. The attachment for the cartilaginous symphysis extended posteriorly to the level of the penultimate premolar, was not medially expanded, and shows no evidence of a symphyseal foramen or connection with Meckel's element.

**Postcanine Alveoli** Only in specimen MPEF-PV 2338 is there an indication of the dimensions of the distal alveolus of the lower canine. This is preserved on the anterior most margin of the specimen as a mesially facing concavity that shows a wider radius of curvature and more lateral extent than the alveoli corresponding to the mesial and distal roots of p1. The state of preservation of the distal canine alveolus precludes further characterization of the structures accommodating the two-rooted lower canine, but allows the confident identification of the first and subsequent premolar loci. The alignment of several edentulous (MPEF-PV 2014, MPEF-PV 2337; Figs. 4 and 5) and tooth-bearing (MPEF-PV 2338, MPEF-PV 2372, and MPEF-PV 2020; Figs. 6, 7 and 8) dentary bone specimens from the La Colonia Formation shows that there is a sum total of 14 postcanine alveoli in the lower jaw. Important features associated with this sequence are the presence of a mental foramen on the lateral

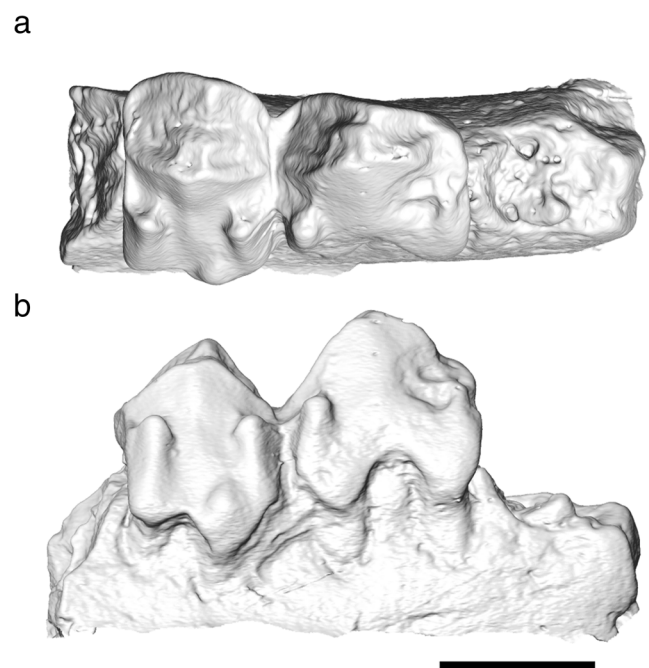


**Fig. 8** *Reigitherium* MPEF-PV 2020. Cast of left dentary fragment (reversed) showing p4 and m1. **a** occlusal view; **b** labial view. Scale bar is 1 mm



dentary surface ventral (or posteroventral) to the fifth alveolus; and a sharp change in alveolar pattern between the eighth and ninth alveolar processes, which is taken to mark the premolar-molar boundary. While the alveoli corresponding to the lower canine are not fully preserved, the anterior most alveolus in this sequence is inferred to be the first postcanine alveolus because of its small size, and location above the shallowest extent of the dentary. It is unlikely that premolar alveoli mesial to the anterior most alveolus preserved in this sequence would be large enough to support an occlusally relevant dental element, if the gradient of distal alveolar size increase is preserved.

The first two postcanine alveoli are interpreted to correspond to the two-rooted lower first premolar. MPEF-PV 2372 (Fig. 7) best preserves these alveoli, and shows the presence of two subequally sized conical roots. Both roots are circular in cross section, with small circular and centrally placed root canals. The first two alveoli, which accommodate these roots, display subequally high medial and lateral margins, and lack any evidence for exodaenodonty (the lateral bulging and overhanging of lower molariform crowns, often associated with labial emargination of corresponding alveoli; Rose 2006). The third and fourth postcanine alveoli correspond to the second lower premolar, as can also be seen in MPEF-PV 2238 and MPEF-PV 2372. These two alveoli are subequal in size, and are only slightly wider mediolaterally than the first and second alveoli. The medial and lateral alveolar margins are also subequal in height, similar to p1.

The fifth and sixth postcanine alveoli are associated with the elongate third lower premolar. These alveoli are mediolaterally wider than the preceding alveoli, and assume a generally ovoid, as opposed to circular, outline. Because of the elongate shape of the p3, the raised interradicular alveolar process between the fifth and sixth alveoli is longer mesiodistally than in any other postcanine tooth position. The space between the fifth and sixth alveoli is also longer than the diastemata between any two preserved tooth positions. The seventh and eighth postcanine alveoli correspond to the ultimate (fourth) lower premolar position, and are similar in size, but are larger and more closely approximated than the alveoli corresponding to p3. The specimens MPEF-PV 2337 and MPEF-PV 2020 (Figs. 5 and 8) show that the lateral alveolar border for these two alveoli is significantly lower than the medial alveolar border. Both the seventh and eighth postcanine alveoli are mediolaterally elongated, but are slightly less ovoid than the preceding two alveoli.

The ninth through 14th postcanine alveoli show an alternating pattern where alveoli corresponding to mesial roots are enlarged and transversely elongate (beyond just being ovoid in cross section) and alveoli corresponding to distal roots are reduced and circular in cross section. This alternating pattern is characteristic of the molars seen in dryolestids and supports the presence of three lower molars in *Reigitherium*. The

known specimens preserving lower molar alveoli are MPEF-PV 2014, MPEF-PV 2020, MPEF-PV 2337, and MPEF-PV 2338 (Figs. 4, 8, 5, and 6). These specimens show some discrepancies in relative alveolar size and degree of emargination of the lateral alveolar borders, which we interpret as intraspecific variation.

The ninth and tenth postcanine alveoli correspond to the lower first molar position, and can be seen in MPEF-PV 2338, MPEF-PV 2020, and MPEF-PV 2337, while only the tenth alveolus is seen in MPEF-PV 2014. All pertinent specimens show the ninth postcanine alveolus to be the widest mediolaterally in the postcanine tooth row, with a lateral alveolar margin much lower than the corresponding medial alveolar margin. Specimens MPEF-PV 2014, MPEF-PV 2020, and MPEF-PV 2338 also show that the tenth alveolus, while much smaller than the preceding alveolus, also extends labially enough to emarginate its lateral alveolar border. The specimen MPEF-PV 2337 shows a tenth alveolus that is smaller, circular in cross section, and more lingually positioned compared with the other specimens mentioned. This prevents the tenth alveolus from having an emarginated lateral margin in MPEF-PV 2337 or from being visible in lateral view; however, a small depression is present lateral to this alveolus which probably accommodated an interradicular rootlet associated with the m1.

The 11th and 12th postcanine alveoli are best preserved in MPEF-PV 2014 (Fig. 4). The specimen MPEF-PV 2337 also preserves the 11th alveolus, but the 12th alveolus is lost due to a major fracture in the specimen. The 11th postcanine alveolus corresponds to the mesial root of m2, and is transversely elongate and emarginated laterally, similar to the ninth postcanine alveolus. The 12th postcanine alveolus corresponds to the distal root of m2, and is approximately two-thirds the mediolateral width of the preceding alveolus. The 12th postcanine alveolus is also more lingually placed and less laterally emarginated than the 11th postcanine alveolus.

The 13th and 14th postcanine alveoli are the smallest in the molar series, and are also thinner mesiodistally and labiolingually than the alveoli corresponding to the third and fourth premolars. The distal two alveoli are visible in MPEF-PV 2014 and MPEF-PV 2337 (Figs. 4-5) and there is some difference in alveolar cross sectional outline implied by these specimens. The smaller dentary fragment MPEF-PV 2014 shows that the 13th postcanine alveolus is mediolaterally elongate and ovoid in cross section, and is succeeded by a smaller and more circular 14th alveolus. The ultimate alveolus seen in MPEF-PV 2014 is much more obliquely set within the mesiodistally directed crest of a raised buttress of bone. The intersection of this raised buttress with the 13th and 14th alveoli is only seen in MPEF-PV 2014, however. The more complete MPEF-PV 2337 also preserves the penultimate and ultimate alveoli, but shows both of these to be more transversely elongate. The ultimate alveolus is also much more

vertically implanted MPEF-PV 2337, and is placed labial to the mesially running buttress on the dentary. Despite these minor topographic variations, these two specimens are of subequal size. Similar variations in the ultimate molar alveoli and root pattern are also present in the larger sample of *Coloniatherium* dentaries from the El Uruguayo locality of the La Colonia Formation (Rougier et al. 2009b; this taxon is present but rare in the sample from the Anfiteatro 1 locality).

While there are no specimens from La Colonia preserving the morphology of the ultimate (third) molar, the conformation of the distal two alveoli in MPEF-PV 2014 and MPEF-PV 2337 demonstrate that the corresponding molar crown would have been significantly narrower than the preceding molars, especially distally. Only MPEF-PV 2337 clearly demonstrates the presence of a retromolar space, mesiolingual to the anterior base of the coronoid process.

### Descriptions of Canine and Postcanine Morphology

The most confusing aspect of the morphology seen in *Reigitherium* is its highly modified dentition. Upper and lower molariform loci show mediolateral elongation associated with the addition of neomorphic structures, and most positions show mesiodistal compression associated with the loss, fusion, and modification of plesiomorphic features compared to the ancestral cladotherian or “eupantotherian” condition (Fig. 3). Among the known Cretaceous meridiolestidans, *Reigitherium* is the most autapomorphic and highly specialized taxon. And its morphology has facilitated an unprecedented variety of opinions regarding the assignment of isolated dental elements to the upper versus lower tooth rows, the orientation of these elements along mesiodistal and labiolingual axes, and the differentiation of left versus right elements. It is not surprising, therefore, that alternative phylogenetic hypotheses based on differing fundamental assumptions of cusp homology have produced a wide variety of opinions regarding the location of *Reigitherium* relative to Mammalia generally.

One remarkable feature found in the dentition of *Reigitherium* is the pervasive development of interradicular crests, which form thin raised ridges or nervure structures from the basal dentine surface between the insertions of the surrounding roots. Interradicular crests have been described in several eulipotyphlan taxa such as erinaceids (Butler 1948) and Caribbean soricomorphs (McDowell 1958), with unknown functional significance. In *Reigitherium* all known upper and lower tooth positions represented by adequately preserved specimens show the presence of a linear or furcating interradicular crest, which supports the attribution of isolated elements to this taxon. Further descriptions of each element known from the La Colonia sample are provided below, but because of their complexity newly discovered diagnostic and heuristic features allowing for the orientation and

identification of the isolated molariform elements in *Reigitherium* are reviewed in the following paragraphs.

The fragmentary dentary described by Pascual et al. (2000) demonstrated the presence of labial cusplids, termed “additional cusps” by these authors, on two molariform tooth positions (here interpreted to be p4 and m1). These structures are here renamed the mesial, distal, and labial accessory cusplids, corresponding to their position on the crown surface. The expanded sample of upper and lower molariform elements described here further demonstrates the presence of neomorphic cusplids on m2 (including mesial, distal, and two labial accessory cusplids), and neomorphic labial cusps on the first and second upper molars as well. These neomorphic cusps/cusplids allow the orientation of the upper and lower molariforms along the mediolateral axis, but do not resolve the right versus left, and upper versus lower identity of isolated dental elements.

The primary central cusps in the molariforms of *Reigitherium* (cusp “a” or protoconid in the lower dentition, cusp “A” or paracone in the upper dentition; Butler 1939; Patterson 1956) are associated with low, sub-linear corrugations that descend from the apex of these cusps to lose distinction among the crenulations present in the primitive trigonid and trigon regions, respectively. These low corrugations show very little relief relative to the underlying crown surface and, because of the lack of high-resolution surface information (such as the 9  $\mu\text{m}$  CT data used here), have not been accurately figured in prior descriptions of *Reigitherium*. Because these linear corrugations are associated with the primitive mammalian “A” and “a” cusps (paracone and protoconid, also termed eocone and eoconid, respectively; Vandebroek 1961), the presence of extended linear corrugations descending from these primitive cusps allows the upper versus lower differentiation of isolated dental elements. This is because of the labial position of the protoconid and lingual position of the paracone in tuberculosectorial or “pre-tribosphenic” dentitions.

The molariform elements of *Reigitherium* can also be oriented mesiodistally because of the wider mesial curvature, compared with distal curvature, of the crown when seen in occlusal view. The wider mesial curvature of upper molars is caused by the more labial placement of the labial terminus of the mesial cingulum relative to the distal cingulum (as seen in several mesungulatoid meridiolestidan species), and the position of the labial most neomorphic cusp (ectostyle) slightly anterior to the transverse midline of the upper crown surface. The upper premolars can also be oriented mesiodistally because of the association of the stylocone with the distal cingulum, which is a characteristic seen in all known mesungulatoid taxa. In *Reigitherium*, because of the more distal placement of the distal cingulum, the stylocone is positioned near the distal margin of the crown in both the penultimate and ultimate upper premolars. While the placement of the stylocone along the distal embrasure is a characteristic unknown in the cheek

teeth of any other trechnotherian taxon, this orientation is justified for the posterior two premolars known in *Reigitherium*, based on comparisons with the morphology known in mesunguloid taxa, and structural relationships with the in situ lower dentition known in the dentary specimen MPEF-PV 2338.

The lower molars can be oriented mesiodistally because of the position of the labial most neomorphic cusplid anterior to the transverse midline of the crown, similar to the upper molars. The lower premolars can be oriented based on their anteriorly skewed profile in lateral view.

## Lower Dentition

**Lower Canine** The specimen MPEF-PV 2347 (Fig. 9c and f) is a robust, double-rooted, and recurved canine. This specimen appears large when compared to the known gracile anterior extent of the dentary bone (seen in the fragmentary specimen MPEF-PV 2372, which lacks canine alveoli, and MPEF-PV 2338; Figs. 6 and 7) but the presence of an interradicular crest within the interradicular arch of this tooth suggest it is referable to *Reigitherium*. Additionally, the presence of a distally-facing attritional wear surface on the concave posterior edge of the canine further suggests that this specimen belongs to the mandibular dentition. The mediolateral width across the

fractured base of the distal canine root (1.90 mm) is approximately twice that of the known width of the dentary bone across the mesial p1 alveolus. However, it appears likely that the distal root tapered significantly before reaching its accommodating alveolus. The ventrodistal extent of the mandibular symphysis also does not show a bulge or inflation in response to the internal commencement of the distal root of the lower canine.

While two roots of the lower canine are not preserved in the isolated canine MPEF-PV 2347, the orientation of the bilobed basal region of the crown indicates that both the mesial and distal roots were procumbent and were most likely concave dorsally. It is also probable that the mesial root is oriented slightly more vertically than the distal root, causing the canine crown to be procumbently situated in the dentary. Underneath the cervical region the interradicular crest connecting the two roots shows a small medially projecting buttress and larger laterally projecting buttress, both of which intersect the mesiodistally oriented interradicular crest at nearly a right angle. The interradicular crest's lateral buttress is labially extended to the labial edge of the crown surface and was possibly enameled to some extent. This makes it appear as though the lower canine possessed three roots in labial view; however, when viewed ventrally it is clear that the lateral buttress does not project far enough ventrally to be considered an independent root or rootlet.

Two thin crests ascend to the recurved apex of the canine from points mesial to the mesial root and distal to the distal root. These two crests give the canine crown a recurved arrowhead shape in lateral view. The distal crest is sharper and a concave surface develops both on its lingual and labial aspects. The unusual shape of the canine in *Reigitherium* appears proportionately very robust and is reminiscent of the lower canine seen in *Necrolestes* (Wible and Rougier 2017). The canine crown is also slightly curved labiolingually, with a concave lingual aspect and convex labial aspect.

**Lower First Premolar** This tooth position is represented by one isolated specimen, MPEF-PV 2368 (Fig. 10). It preserves a complete, and relatively unworn, crown surface but no cervical or root features. This element is referred to here as p1, but may reasonable be homologized with the deciduous p1, which is the first permanent premolar seen in most extant plesiomorphic therian mammals (Lockett 1993). At present we have no data to help us choose between these options.

The first lower premolar is mediolaterally thinner than any other postcanine position known in *Reigitherium*, being approximately 1.31 mm wide and 2.44 mm long mesiodistally. The single cusplid is located over the base of the mesial root, giving it a procumbent triangular profile in lateral view. The occlusal edge of the lateral profile is formed by a thin crest. From the apex of the central cusplid this crest descends along a steep parabolic curve mesially, and along a shallower

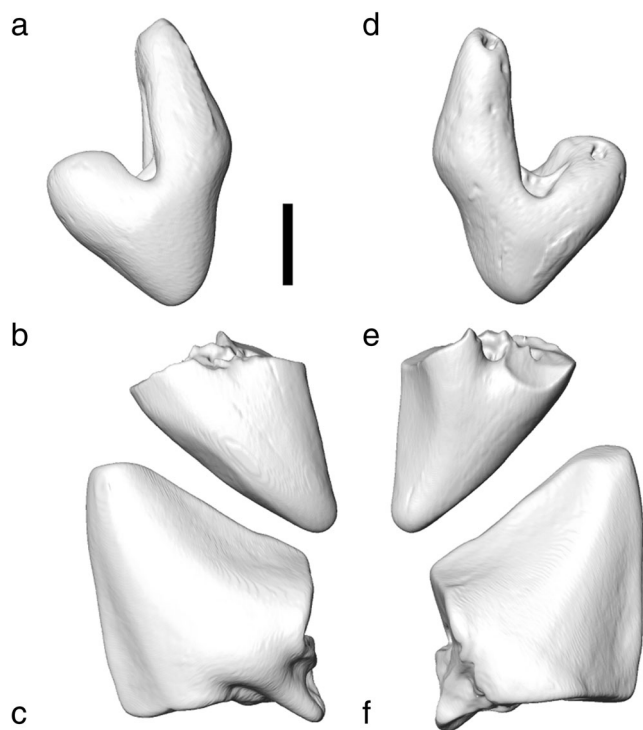


**Fig. 9** *Reigitherium* upper and lower canines positioned to show morphological correspondence and contact between opposing crown surfaces. **a,d** MPEF-PV 2349 upper canine (reversed); **b,e** MPEF-PV 2375 tip of upper canine (reversed); **c,f** MPEF-PV 2347 tip of lower canine. **a,b,c** labial view; **d,e,f** lingual view. Scale bar is 1 mm

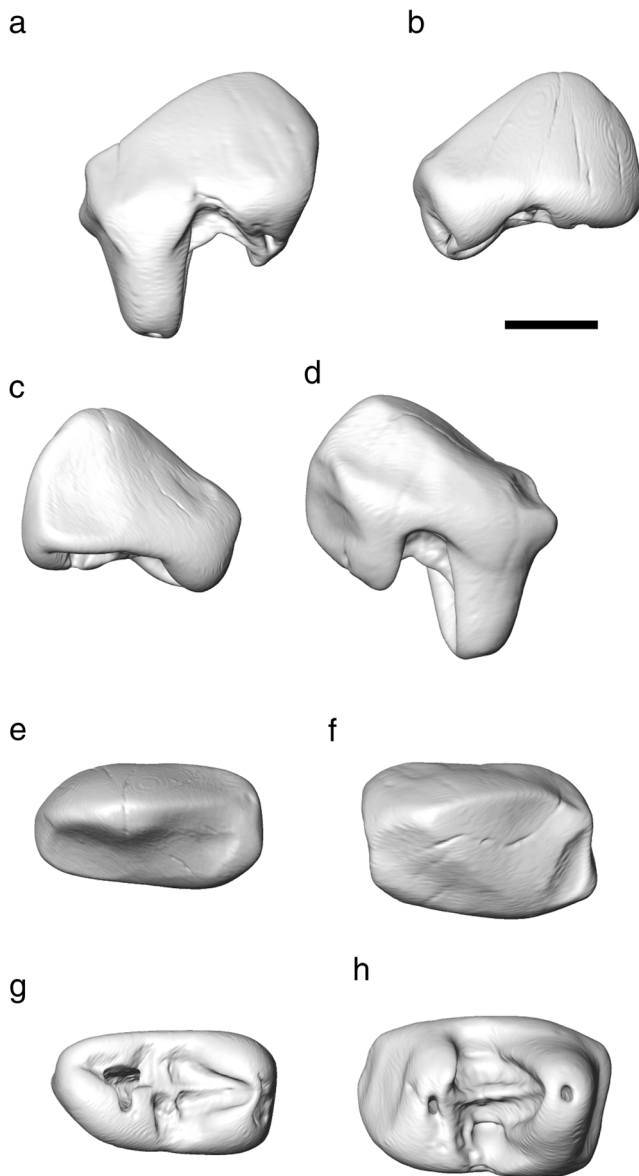


**Fig. 10** *Reigitherium* first and third lower premolars. **a,d,f,g** MPEF-PV 2376 lower right p3; **b,c,f,g** MPEF-PV 2368 lower right p1. **a,b** labial view; **c,d** lingual view; **e,f** occlusal view; **g,h** ventral view of roots and interradicular crests. Scale bar is 1 mm

straighter curve distal to the central cuspid. The outline of the crown in occlusal view is generally ovoid, similar to the two succeeding premolars, and lacks any mesial or distal emarginations or interstitial wear surfaces.

**Lower Second Premolar** This element is best preserved in the dentary specimen MPEF-PV 2372 (Fig. 7). This is an anterior left dentary fragment with two alveoli preserved for the lower p1, a complete in situ p2, and the mesial half of the lower p3 in situ. The lower second premolar shows a low, broad, unicuspid crown surface with the apex of the main cuspid (protoconid) placed over its mesial root. This gives the entire crown a mesially skewed triangular profile in lateral or medial

view. The posterolingual aspect of the crown supports a poorly defined attritional wear surface.

Lingually, the Dentine Enamel Junction (DEJ) forms two hemispherical lobes that overhang medially the supporting roots. The lingual surface of the crown above these small lobes is fairly smooth, featureless, and vertically oriented. Labially, the DEJ forms a deep interradicular incisure between the mesial and distal roots, which interrupts the labial extension of the DEJ on the lateral aspects of the mesial and distal roots. The lateral rims of the alveolar processes are also proportionally lower than the medial rims to accommodate these lateral extension of the DEJ. In occlusal view the outline of the p2 is generally ovoid, being approximately 2.41 mm long mesiodistally and 1.46 mm wide labiolingually.

The distal surface of p2 forms a distally dipping slope of approximately 33 degrees, ending in a small, horizontal cingulid over the DEJ. The mesial surface of p2 is smoothly convex and mesially facing. However, the basal most extent of the mesial surface is emarginated (indented) to accommodate the distal heel of the preceding (p1) tooth position. This emargination forms a slight ventromesially facing concavity.

The two roots in p2 can be seen in the micro-CT images of MPEF-PV 2372. Both mesial and distal roots are robust, cylindrical, and vertically implanted in their respective alveoli. A mesiodistally directed interradicular crest under the cervix connects both roots.

**Lower Third Premolar** This tooth position is best preserved in the MPEF-PV 2338 (Fig. 6) fragmentary dentary specimen. Fragments of the crown surface are also known in MPEF-PV 2372 (Fig. 7) and several other isolated teeth (e.g. Fig. 10). As in the preceding tooth position, the apex of the main cuspid on p3 is located above the mesial root. However the extent of mesial skewing of the p3 crown is much less apparent than in the p2, giving the silhouette of the crown the shape of a blunt arch in lateral and medial views. The p3 is slightly smaller in most dimensions than the preceding tooth, being 2.31 mm long mesiodistally, and 1.38 mm wide labiolingually in MPEF-PV 2338.

The mesial aspect of the p3 shows a sharp crest ascending from a thin mesial cingulid over the mesial root, and intersects the apex of the main cuspid (protoconid). There is a considerable amount of attritional wear medial to this crest on MPEF-PV 2338; however, it is apparent that this crest continues distally on to the posterior aspect of the crown, ending in a slightly larger distal cingulid. The surface of the crown medial and lateral to this longitudinal crest smoothly curves towards the longitudinal midline in the mesial half of the tooth, giving the mesial half of the crown a blade-like appearance. The crown surface medial and lateral to the longitudinal crest forms a flat, posteriorly-facing, vertical wall above the distal root of the tooth. The distal most region of the p3 forms a mediolaterally wide but short distal cingulid.



The DEJ forms labial extensions of the crown surface over both the mesial and distal roots. These extensions are separate at their base, and so do not form a discrete exodaenodont lobe. Additionally, they are both smoothly convex and lack any expression of labial cuspids. Lingually, the DEJ also forms two hemispherical lobes over the mesial and distal roots. The hemispherical lobe over the distal root is slightly more ventrally extensive. Both roots extend vertically into their respective alveoli. As in the preceding tooth position, the two roots are connected by a single, straight interradicular crest. In MPEF-PV 2338 there is no expression of a lingually placed accessory rootlet, or extension of the interradicular crest, as figured for this tooth position in Pascual et al. (2000).

**Lower Fourth Premolar** Known from specimens MPEF-PV 2020 and MPEF-PV 2338 (Figs. 6, 8 and 11), the p4 is a molariform ultimate premolar, longer mesio-distally than wide labiolingually, unlike the succeeding molars. The maximal mesiodistal lengths and labiolingual widths average 2.28 mm and 1.73 mm, respectively.

We adopt the hypothesis (Rougier et al. 2011, 2012) that this element represents the ultimate premolar, as opposed to the first molar, as suggested by Pascual et al. (2000). This discrepancy in dental formula and attribution is based on our comparisons with the morphologically closest dental elements in *Peligrotherium*, and to a lesser extent *Coloniatherium* (see Figs. 1 and 2). The molariform tooth inferred to be the

ultimate premolar in *Peligrotherium* has accumulated much less premortem wear, compared with the three lower molars contained in the exceptionally preserved specimen described by Paez-Arango (2008). This suggests that the tooth in this position had erupted later than its succeeding tooth, and therefore it is likely a successor (as opposed to a first-generation) tooth. Therefore, despite its complexity, we attribute this element to the p4 locus based on its correspondence to the ultimate lower premolar in *Peligrotherium* (based on its inferred replacement pattern) and the alveolar pattern at this location (described above).

The lingual half of the p4 crown in *Reigitherium* shows the plesiomorphic tuberculosectorial morphology of the premolar crown, which has been modified by crenulation of the region representing the trigonid basin. These features are most clearly presented in the dentary specimen MPEF-PV 2338, with the transversely approximated protoconid and metaconid being clearly visible despite a minor amount of apical wear present on the apex of the protoconid. Anteriorly, the paracristid can be recognized as a salient crest descending mesially from the apex of the protoconid and intersecting with a minor swelling that represents the reduced paraconid. Mesial to the paraconid swelling, the paracristid continues without interruption into a tortuous pre-paraconid crest, which abruptly deflects lingually before itself seamlessly blending into the lingual commencement of the mesial cingulid. Beside the paracristid, several linear wing-like crests can be seen to descend from the apex of the protoconid and metaconid, giving these trigonid cuspids a selenodont-like appearance.

Distal to the protoconid an indeterminate crest (possibly representing the homolog of either the labial half of the protocristid or the cristid obliqua) descends along a direct distal route to terminate just mesial to the distal cingulid. The metaconid has a similar distal crest, with similarly uncertain homology, that descends distolingually before blending seamlessly into the lingual commencement of the distal cingulid. The ultimate lower premolar of *Reigitherium* therefore shows an association of the primary trigonid cusps with the mesial and distal cingulids, a condition that is further accentuated in the lower molars. However, unlike them the ultimate lower premolar still preserves a complete and lingually open trigonid. Also, unlike the molars, the distal margin of the trigonid is wider than the mesial margin. This creates a gradual transition between the mediolaterally compressed premolar morphology and the transversely widened morphology seen in the molars. The lack of closure of the p4 trigonid is the result of the relatively low and shortened form of the crest descending mesially from the metaconid, which loses distinction before being able to blend with the lingual commencement of the mesial cingulid.

The labiolingually thinner region enclosed by the trigonid basin mesial to the protoconid suggests that a molariform upper tooth did not contact the mesial edge of p4 or the

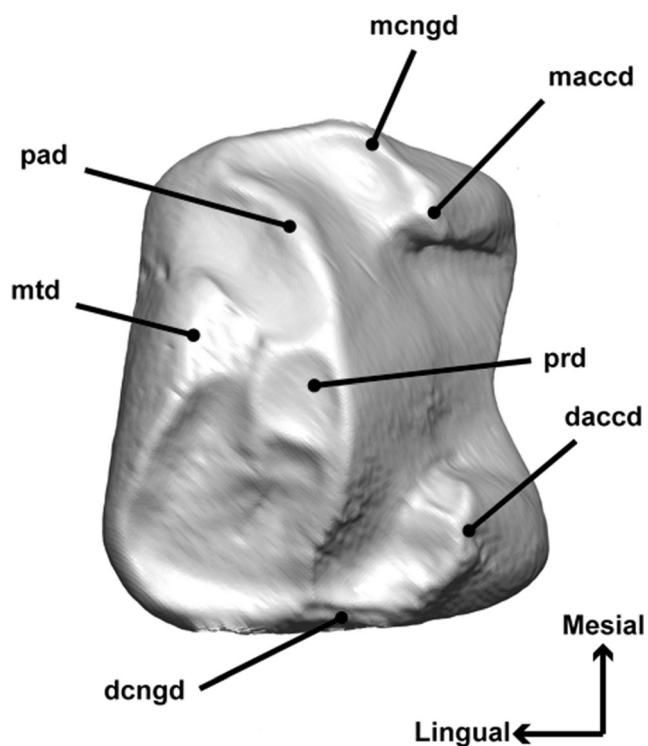


**Fig. 11** *Reigitherium* lower p4 in MPEF-PV 2338 showing modified trigonid cusps; pad, paraconid; prd, protoconid; mtd, metaconid; mcngd, mesial cingulid; dcngd, distal cingulid

embrasure anterior to it. This can be seen as indirect support for the lack of complete molarization in the tooth corresponding to the upper third premolar.

The labial half of p4 forms a smoothly convex lateral slope descending from the labial aspect of the trigonid, supporting two accessory cusplids. These cusplids are small but fairly conical (the mesial cusplid is damaged in the specimen MPEF-PV 2020), and form the labial termini of the mesial and distal cingulids, respectively. Small frenular crests also connect these cusplids with the lateral aspect of the trigonid, independently of the sharp apical boundaries of the mesial and distal cingulids.

The base of the crown extends further ventrally beneath the mesial and distal margins of the tooth, forming a slight interradicular arch, visible labially. The labial surfaces of the two labiolingually extended roots of this tooth are also visible in lateral view. The lingual surface of the p4 crown forms a fairly flat and featureless sheet oriented in a parasagittal plane. The mesial and distal cingulids do not have any expression on this surface, and the interradicular arch is much shallower in lingual view.

Both roots are expanded mediolaterally at their attachment to the tooth cervix, but deflect labially and taper to have a cylindrical cross section as they extend deeper into their respective alveoli. The apical foramina for both roots are located diametrically opposite the surface expression of the labial cusplids on the crown. The mesial root is slightly convex along its mesial aspect, but vertically implanted into its alveolus. The distal root is slightly inclined posteriorly (approximately 10 degrees from vertical).

**Lower First Molar** The transitional morphology presented by the ultimate lower premolar provides a valuable schematic for interpreting the complexity of the succeeding dentition. In particular, the morphology of the lower molars can be understood as having been derived from the condition seen in the p4 by the further extension and definition of the crest connecting the mesial aspect of the metaconid with the lingual commencement of the mesial cingulid; and the reduction of the paraconid swelling, or its appression onto the metaconid (making this composite structure technically an amphiconid; Yardeni 1942; Patterson 1956). With the confluent connection between the crest descending mesially from the metaconid to the mesial cingulid, a continuous raised loop is developed that circumscribes the crenulated enamel of the trigonid basin. This structure is termed here the *enceinte* (see Fig. 3b), and is formed from the contiguous circuit of the paracristid, mesial cingulid, mesial crest of the metaconid, distal crest of the metaconid, distal cingulid, and distal crest of the protoconid. The architectural usage of the word *enceinte* refers to the main defensive line of wall towers and curtain walls surrounding a castle or other fortified location, which is closely analogous to the conformation of trigonid cusplids and crests seen in this

element. An *enceinte* is apparent on both known lower molar loci in *Reigitherium* (m3 is unknown), and is vertically highest anteriorly near the trigonid cusplids. Within the boundaries of the *enceinte* the crown enamel is highly ornamented and (as mentioned by Pascual et al. 2000) contains a mesiodistally oriented sulcus separating the bases of the protoconid and metaconid. The homology of this sulcus is ambiguous, and may correspond to the indentation of the protocristid, or the center of the trigonid basin seen in the lower molars of other meridiolestidan taxa.

The crown of the lower first molar is known in situ from two dentary specimens (MPEF-PV 2020 and MPEF-PV 2338; Figs. 6 and 8) and from a single isolated specimen (MPEF-PV 2317; Fig. 12). Each of these m1 specimens show a complex crown surface, with minor individual variations, but are all wider labiolingually (average 2.57 mm) than mesiodistally (average 1.73 mm). The lingual half of the crown surface contains the trigonid region, enveloped by an ovoid *enceinte*. The apex of the protoconid in this region can be seen as a small conical projection independent of the labial wall of the *enceinte*. Internal to the *enceinte* the surface of the protoconid shows several low corrugations, two of which run

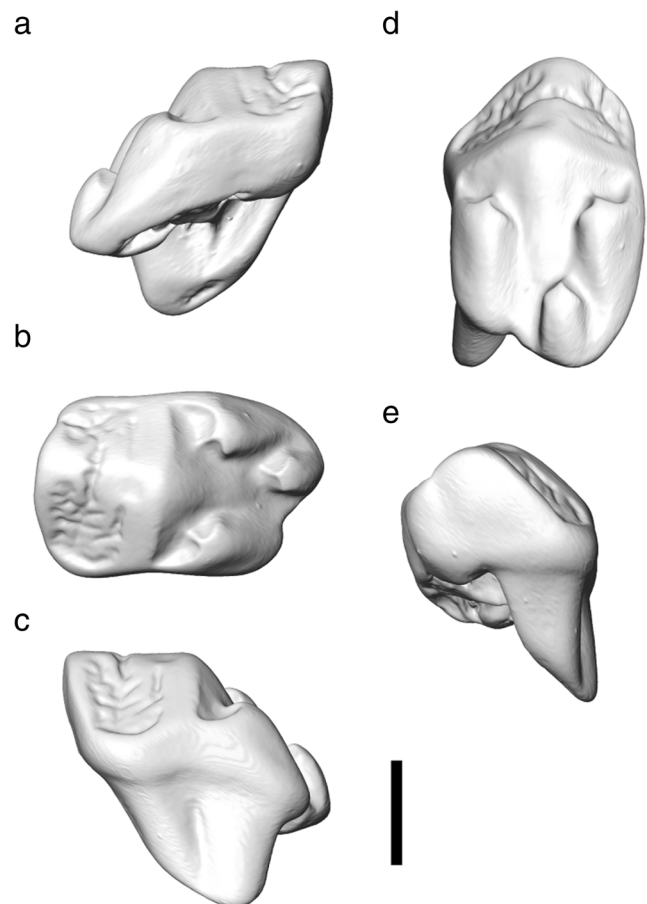


**Fig. 12** *Reigitherium* lower right first molar MPEF-PV 2317. **a** mesial view; **b** occlusal view; **c** distal view; **d** dorsolabial view; **e** lingual view. Scale bar is 1 mm

mesially and distally, respectively, and lose definition among the other crenulations of the trigonid region. A third short corrugation runs labially from the protoconid and terminates into the lingual side of the labial portion of the enцеinte.

The paraconid is absent in both known lower molar positions in *Reigitherium*. As mentioned above, this is the result of the paracristid being incorporated into the mesial border of the enцеinte with the concomitant reduction of the paraconid itself, or its lingual displacement and seamless fusion with the metaconid. The metaconid in m1 is not independent of the lingual wall of the enцеinte, which attaches to this cuspid slightly lingual to its apex. Other than this attachment, the metaconid does not show the expression of elongate corrugations like those seen on the protoconid, but is also highly crenulated.

The two trigonid cusps, and the regions of the enцеinte immediately labial and lingual to them, are the highest features of the crown surface. This elevated region forms a mediolaterally directed guiding-ridge, which would have helped to limit motion of the mandible to horizontal translation near centric occlusion. There is also a thin, anterior-posteriorly directed sulcus centrally placed between the protoconid and metaconid; however, this depression is so thin and shallow that it would not have altered the function of the guiding-ridge of the trigonid, which it intersects.

The labial half of the lower first molar is an exodaenodont lobe embellished with several accessory cuspidulids. The exodaenodont lobe extends the crown's lateral margin further labially and ventrally than the preceding premolar, and completely obscures the inter-radicular arch and lateral aspect of the roots from lateral view. Similar to the preceding premolar, two cuspidulids are placed in the anterior and posterior margins of this lobe and form the labial terminations of the mesial and distal cingulids, respectively. These cuspidulids are not as labially positioned as those seen in the ultimate lower premolar, but like the p4 these cingulid cuspidulids show lingually directed frenular crests connecting to the lateral aspect of the exodaenodont lobe.

The basal margins of the mesial and distal cingulids project further laterally than their corresponding apical margins, which terminate laterally at the accessory cuspidulids described above. This causes the labial aspect of the mesial and distal cingulids to form low, lateroventrally directed buttresses in the intervening space between the cingulid-terminating cuspidulids and the lateral border of the crown surface. A third lateral cuspidulid is located on the labial margin of the exodaenodont lobe, independent of the cingulids and placed slightly anterior to the transverse midline of the crown. As with the other cuspidulids, a frenular crest projects medially for a short distance from this lateral most cuspidulid as well. Ventrally, the inferior extent of the DEJ is deeper under this third cuspidulid than elsewhere on the tooth. The lingual surface of the crown is a vertically directed, featureless sheet similar to the condition seen in the preceding tooth position.

The two roots in this position can be seen to extend approximately 2.8 mm into the alveolar sockets in MPEF-PV 2338. The lingual and labial aspects of both roots form a labially convex curve, and both roots become thinner and more circular in cross section as they taper towards small apical foramina. The mesial and distal apical foramina are located diametrically opposite the apices of the mesial and distal cingulid cuspidulids, respectively. Near the cervical region of the m1, both roots fan out lingually to give the base of their insertion into the cervix a transversely elongate cross section. A single, straight interradicular crest connects the mesial and distal roots beneath the m1 cervix. The mesial root is noticeably more robust and vertically implanted than the distal root. The distal root is more gracile and posteriorly inclined by approximately 11 degrees.

**Lower Second Molar** This element is best known in MPEF-PV 2237 (Fig. 13), an isolated tooth showing some premortem apical wear, obscuring several locally elevated features. This specimen is inferred to represent the m2 because of the greater discrepancy between the mediolateral width between its mesial and distal borders, and the size of its mesial and distal roots. This tooth is unlikely to represent the crown morphology of the currently unknown m3 of *Reigitherium*, because of the obvious mismatch between its dimensions and the size and positioning of the distal two alveoli, known in MPEF-PV 2014 and MPEF-PV 2337. The m2 is approximately 1.75 mm long mesiodistally, and 2.67 mm wide labiolingually.

The trigonid region is composed of an elevated protoconid and metaconid. Wear on the protoconid prevents the presence

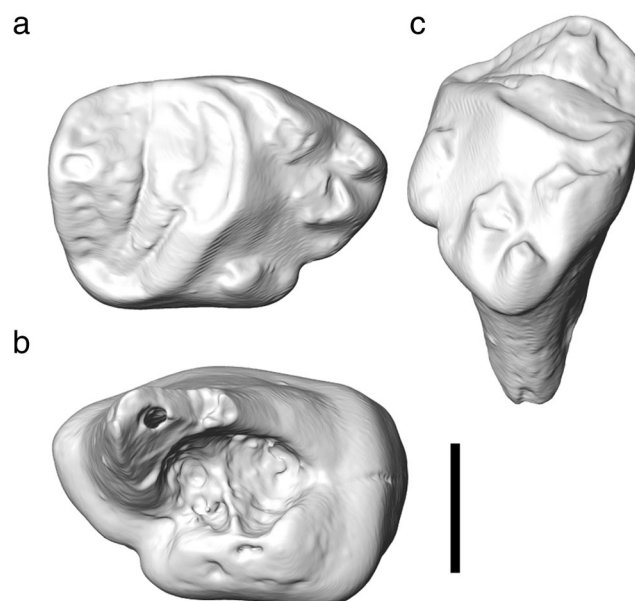


**Fig. 13** *Reigitherium* lower right m2 MPEF-PV 2237. **a** occlusal view; **b** ventral view of roots and interradicular crest; **c** dorsolabial view. Scale bar is 1 mm

of anteroposteriorly or labially directed corrugations from being evaluated; however, there is still a prominent guiding-ridge connecting the protoconid to the metaconid. Also, as in the preceding molar, there is also an anteroposteriorly directed sulcus intersecting this ridge. As in the m1, the apex of the metaconid participates in the formation of the medial border of the encephale.

The labial termini of the cingulids are elevated into cusplids on the lingual border of the exodaenodont lobe. The labial border of the exodaenodont lobe has two additional accessory cusplids, which are unassociated with either cingulid. The labial most cusplid extends the DEJ ventrally beneath it. The other accessory cusplid, which does not labially bound either cingulid, is positioned near the lateral border of the exodaenodont lobe, posteromedial to the labial most cusplid. This second accessory cusplid seems more likely to be the serial homolog of the labial most accessory cusplid on m1, because of its similar position adjacent to the lateral aspect of the exodaenodont lobe and lateral buttress of the mesial cingulid. The lingual aspects of all four accessory cusplids also show small frenular crests running lingually from their respective positions.

The mesial root of MPEF-PV 2237 is preserved to a much greater extent than the distal root. However, it is apparent that the mediolateral width of the distal root is at most two-thirds the width of the mesial root, and that it is positioned directly under the distal cingulid. The mesial root of MPEF-PV 2237 shows similar features to the distal root of the m1 specimen MPEF-PV 2317, except that the root canal in MPEF-PV 2237 is much more circular in cross section and labially placed below the lateral projection of the exodaenodont lobe. The distal surface of the mesial root has a wide, vertically oriented groove, the concavity of which is enclosed by medial and lateral expansions of the base of the root. The mesial surface of the mesial root is much less indented by a shallow vertical groove. The lingual surface of the mesial root is obliquely slanted ventrolabially, and is mesiodistally thinner than the labial surface of the mesial root, which is vertically directed. The lateral surface of the mesial root is smoothly convex in a horizontal plane, and is positioned under the lateral projection of the exodaenodont lobe.

## Upper Dentition

**Upper Canine** The two specimens referred to this position, MPEF-PV 2375 and MPEF-PV 2349 (Figs. 9a–e), show a considerable amount of postmortem damage. The crown specimen MPEF-PV 2375 has avoided postmortem abrasion (although it is fragmentary), and better demonstrates original crown morphology to the extent that it is preserved. However, MPEF-PV 2349 preserves a larger fraction of the root structure of the upper canine, but is significantly rounded by postmortem abrasion and erosion. These specimens are

inferred to represent the upper canine, because of the presence of a flattened premortem wear surface on the mesial aspect of MPEF-PV 2375, which would be produced against the distal face of the lower canine.

The two-rooted upper canine crown is mediolaterally compressed but still conical in general form. The apex is positioned over the distal root, giving the crown a recurved profile in lateral view, which is more gracile than in the lower canine. The apex of the canine extends approximately 2.36 mm above the interradicular arch.

The distal root forms a bulge, or heel, near its commencement on the crown surface. The commencement of the mesial root does not alter the convex curvature of the crown's mesial aspect. Unlike in the lower canine, both roots preserved in MPEF-PV 2349 are vertically oriented and cylindrical. An interradicular crest is visible running mesiodistally between the two roots; however, there is no laterally placed rootlet projecting from the interradicular crest as seen in the lower canine.

**Upper Third Premolar** The putative penultimate upper premolar is only known in MPEF-PV 2339 (Fig. 14), an isolated crown lacking any attached cervical or root structures. The crown morphology is largely influenced by a single centrally placed central cusp (paracone), and a smaller parasitic stylocone. This morphology makes orientation of the P3 with respect to the major anatomical axes particularly challenging. However, based on the criteria described above, the inferred distolabial position of the stylocone allows the life position to be estimated. The P3 in *Reigitherium* shows several detailed similarities to the penultimate premolars known in *Peligrotherium* and *Coloniatherium*, such as its triangular occlusal outline formed by a small mesial cingulum and transversely wide distal cingulum. The enlarged distal cingulum is more extensive than in the other mesungulatoid taxa mentioned, commences lingually near the transverse midline of the crown, and is terminated labially by merging with the stylocone. The small mesial cingulum is also comparatively more transversely extensive in *Reigitherium*, and forms a hemispherical arc around the mesial half of the crown. This gives the penultimate premolar a maximal labiolingual width of approximately 2.0 mm, and a mesiodistal length of 2.64 mm.

The large central paracone is flanked by several linear corrugations descending linearly from its apex. Two more salient crests descend mesiolabially and distolabially from the apex as well, with the mesiolabial crest terminating indistinctly near the basal portion of the mesial aspect of the paracone. The distolabial crest descends along the distolabial flank of the paracone to meet a mesiolingually directed frenular crest projecting from the stylocone.

**Upper Fourth Premolar** The morphology of the ultimate upper premolar in *Reigitherium* is known from three specimens



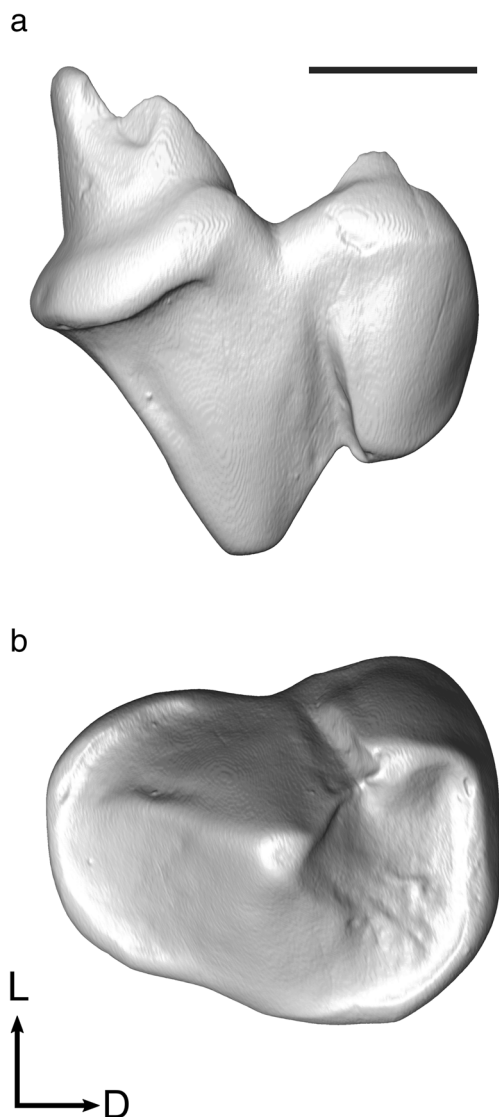


**Fig. 14** *Reigitherium* upper right third premolar (reversed) MPEF-PV 2339. **a** labial view; **b** occlusal view. Mesial is towards the left. Scale bar is 1 mm, and is for a and b. Directional arrows for b only, L - Labial, D - Distal

(MPEF-PV 2341, MPEF-PV 2344, and MPEF-PV 2072; Fig. 15). Only one of these (MPEF-PV 2072) preserves enough of its original morphology to provide reliable measurements, being 1.89 mm mesiodistally and 3.01 mm labiolingually. While each of these specimens show a significant amount of rounding and fragmentation, the major features — an enlarged central cusp (paracone) and a distally placed stylocone — are consistent. Mediolateral elongation and the association of the stylocone with the distal cingulum are characteristics seen the molars and molariform premolars in mesungulatoid meridiolestidans, and these elements in particular are inferred to represent P4 based on the mesial deflection of the lingual lobe of the crown. This mesial deflection is also seen in the ultimate premolars of *Peligrotherium* and *Coloniatherium* (Fig. 1), as opposed to the direct mediolateral

or distally deflected, conformation of the lingual lobe in the true molars. There is also a reasonable mechanical correspondence between MPEF-PV 2072 and the embrasure between p4 and m1 in specimen MPEF-PV 2338 (although these specimens represent different stages of wear).

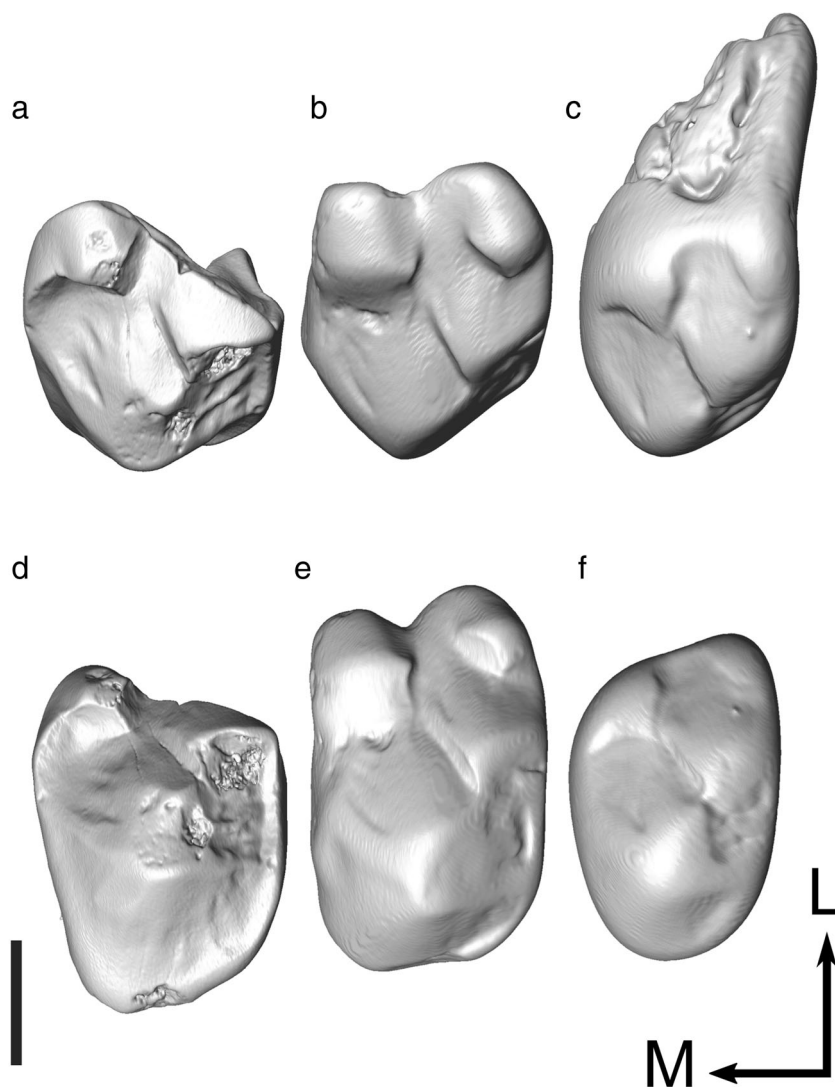
In *Reigitherium* and other mesungulatoid taxa the ultimate premolar is the largest element of the upper tooth row. Specimen MPEF-PV 2072 shows that the P4 contains a large central cusp, similar to the preceding premolar position, and two labial cingular cusps. However, the fourth upper premolar shows much lower crenulations on its occlusal surface, and has a very indistinct and intermittent cingulum. The ultimate upper premolar also shows a small stylocone on the distolabial flank of the large central cusp, approximately halfway between the apex of the central cusp and the distal cingular cuspsule.

The base of the paracone is generally ovoid, and wider labiolingually than mesiodistally, with a centrally placed apex. The centrifugal corrugations on this cusp are very indistinct, partially resulting from taphonomic abrasion in all specimens; they are more apparent but still small in MPEF-PV 2344. The apex of the central cusp shows a distinct, indirect crest connecting with the apex of the stylocone. The stylocone also shows two subsidiary crests running along its mesiolabial and distolabial aspects. Damage to the basal crown in all specimens prevents identification of the number and orientation of roots at this tooth position.

**Upper First Molar** Because of the observable distal gradient of decreasing width in the upper molars of *Peligrotherium*, the specimen MPEF-PV 2238 (Fig. 16a and d) is inferred to represent the upper first molar in *Reigitherium* because of its greater width (3.11 mm) than the specimen inferred to represent the M2 position. However, the morphology of MPEF-PV 2238 has been obscured because of heavy wear and the fact that much of its crown surface can only be inspected using photographs and cast specimens, with most of the primary trigon region having been sacrificed as part of the enamel microstructural analysis reported by Wood and Rougier (2005: fig. 5). While the photography and cast replicas obscure some of the finer features of the original crown surface, it is still apparent that the M1 is elongate labiolingually, with the lingual two-thirds of the crown composed of the primary trigon region. Root structure for this tooth position also cannot be described.

**Upper Second Molar** Two specimens, MPEF-PV 2343 and MPEF-PV 2341 (Fig. 16b–e and f), are inferred to represent the M2 in *Reigitherium* based on their thinner mediolateral width (2.95 mm and 2.71 mm, respectively), compared with MPEF-PV 2238 the inferred M1. The distance in the occlusal plane between the apex of the paracone and stylocone is also smaller in MPEF-PV 2343 (0.89 mm) and MPEF-PV 2341

**Fig. 15** *Reigitherium* ultimate upper premolar morphology as preserved in three different isolated dental specimens. **a,d** MPEF-PV 2344 (reversed); **b,e** MPEF-PV 2072 (reversed); **c,f** MPEF-PV 2373 (reversed). These specimens demonstrate the variable extent of postmortem abrasion seen in La Colonia microfossils. **a,b,c** labial view. **d,e,f** occlusal view. Mesial is towards the left. Scale bar is 1 mm, and is applicable to all specimens. Directional arrows are for d,e,f only, L - Labial, M - Mesial



(1.06 mm) than in the M1 specimen (1.29 mm). While both M2 specimens described above are isolated teeth, the damaged basal region of MPEF-PV 2341 and postmortem rounding of MPEF-PV 2343 make each specimen an appropriate representative of different aspects of the M2 anatomy. As such, all features of crown morphology are based on MPEF-PV 2341, while cervical and root features are based on MPEF-PV 2343. Additionally, as much of the morphology of the known M1 specimen in *Reigitherium* is obscured, most of the characterizations of the M2 morphology described below are likely applicable to the M1 as well.

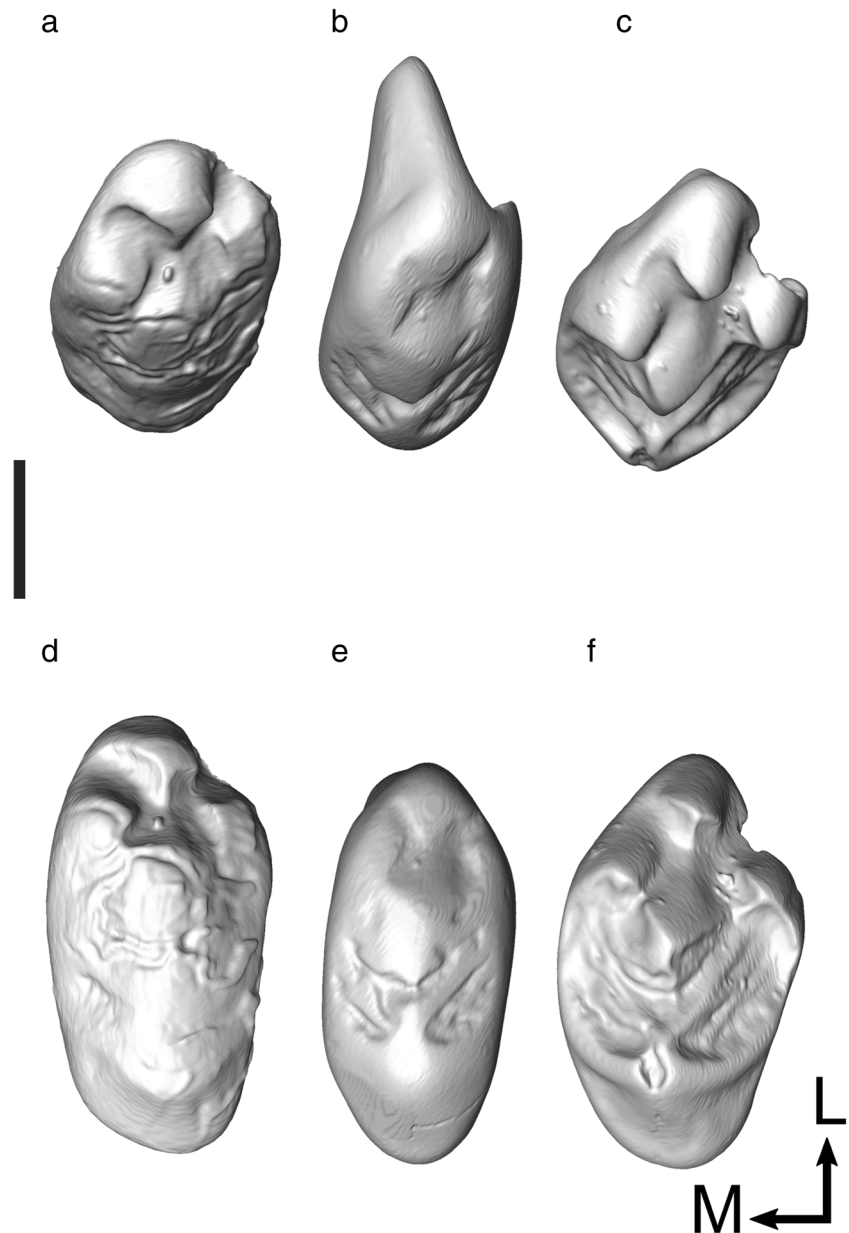
The buccal one-third of the molar crown is composed of the labially extended lateral slope of the stylocone, with three labial cusps partially connate with its surface. These labial cusps mirror the arrangement of the labial cuspidids on the lower molars, but are too low to have come into occlusal contact. The labial most cusp is here termed the ectostyle (based on Hershkovitz 1971) and forms the buccal terminus of a small mesial cingulum, which is indistinct further

lingually. A short, lingually direct frenular crest descends from the ectostyle to merge indistinctly into the lateral surface of the stylocone.

The mesial most cusp is a parastyle; the cusp is at the labial end of the preparacrista and has a minute frenular crest that is partially obscured by wear. The distal most styler cusp is the metastyle, and similar to the parastyle, forms the labial termination of the postparacrista. The frenular crest projecting from the metastyle is slightly longer and more salient than the other frenular crests seen in M2. The metastyle itself is smaller and lower than the other styler cusps, and blends with an indistinct distal cingulum on the lingual portion of the molar crown. The small mesial and distal cingula do not meet labially, and a small cleft is formed on the molar crown between the parastyle and metastyle.

The lingual two-thirds of the crown show two subequally large cusps, the paracone lingually and stylocone labially. The paracone is the only cusp in MPEF-PV 2341 to show any degree of apical wear; however, this does not obscure the

**Fig. 16** *Reigitherium* upper molar morphology. **a,d** cast of MPEF-PV 2238 upper first molar; **b,e** MPEF-PV 2343 possible upper second molar (reversed); **c,f** MPEF-PV 2341 upper second molar (reversed). The close similarity between hypothesized first and second upper molars is apparent, as well as the variable preservation quality seen in the La Colonia material. **a,b,c** ventrolabial view; **d,e,f** occlusal view. Mesial is towards the left. Scale bar is 1 mm and is for all specimens. Directional arrows are for d,e,f only, L - Labial, M - Mesial



strong preparacrista and postparacrista, which extend from its apex (although, see below for an alternative interpretation of these crests). The preparacrista and postparacrista take a hemispherical course from their lingual origin on the paracone, and become confluent with the mesial and distal cingula, respectively, along the middle one-third of their extent. The paracristae detach from the cingula to curve labially into the parastyle or metastyle, respectively.

Lingual to the paracristae the paracone forms a shallow but featureless lingual slope towards the indistinct lingual confluence of the mesial and distal cingula. Labial to the paracristae the lateral slope of the paracone shows several crenulated linear corrugations running toward the base of the stylocone on both its mesial and distal aspects. The paracristae thus

circumscribe a region of ornamented enamel within the primary trigon, which matches the enceinte structure formed from the trigonid on the lower molariform teeth. The apex of the stylocone does not have linear corrugations associated with it; however, two more salient crests can be seen to descend labially, terminating abruptly beneath the parastyle and metastyle, respectively.

The cervical region and roots corresponding to the M2 are only preserved in specimen MPEF-PV 2341. Three roots can be clearly identified for this tooth, each buttressed by a limb of a “Y” shaped compound interradicar crest. Each limb of the tripartite interradicar crest is similar to the single mesiodistally oriented interradicar crests found on the lower molars. A mesiolabially directed branch of the interradicar

crest contacts the mesial root along its lingual edge. While a lingually-oriented branch contacts the lingual root along the center of its labial surface, and a distolabially-oriented branch contacts the distal root along the center of its mesial surface. The contact between all three branches is positioned under the space between the paracone and stylocone.

The mesial root of the M2 is approximately triangular in outline, with a vertical root canal located opposite the lateral preparacrista and parastyle on the crown surface. This root is flattened mesiolabially-distolingually, with a convex mesiolabial surface and concave distolingual surface. The distal root is mediolaterally elongate, and located centrally beneath the distal border of the crown surface. The lingual root has a concave labial surface and convex lingual surface, both vertically oriented.

An alternative hypothesis regarding the homology of what are here termed paracristae is that these structures represent the vertically extended and lingually coalesced mesial and distal cingula. In *Reigitherium* the paracone is labially thickened (Fig. 3a) and the morphology around it shows a convergence of corrugations. If the mesial and distal borders of the upper molars were to be interpreted as full height cingula that have essentially merged with the trigon, the subdued topology of the center of the crown should be seen as the homolog of the primitive dryolestoid upper molar. If this is the case, it would explain the lack of expression of cingula on the lingual surface of the paracone; and would be in greater agreement with the hypertrophied cingular morphology seen in the other known mesungulatoid meridiolestidans. Under this interpretation the paracristae would possibly be homologous to several of the more salient corrugations descending labially from the apex of the paracone, or have lost distinction altogether. A similar morphology is present, although not as highly developed, in *Peligrotherium*, where the cingula approach the trigon level; however, both cingula and the primary trigon persist as distinct features of the upper molars. While this interpretation is plausible and compatible with the available evidence, it is not adopted in the following discussion because of the lack of vertically enlarged cingula in the known premolars of *Reigitherium*, and the ambiguity and capriciousness in identifying trigon and cingular homologs in these highly derived upper molars. The scheme adopted here is simpler and does not vitiate the interpretation of *Reigitherium* as a close relative of *Peligrotherium*, which would only be strengthened if the alternative is adopted.

**Upper Third Molar** This tooth position is only known from MPEF-PV 2369 (Fig. 17), a fragmented isolated tooth missing approximately the lingual one-third of its crown surface, but showing only minor abrasion. The mesiodistal length of the M3 is 1.67 mm, labially across the stylocone; and the apices of the paracone and stylocone were separated by approximately 1 mm. This specimen is inferred to be the ultimate upper molar

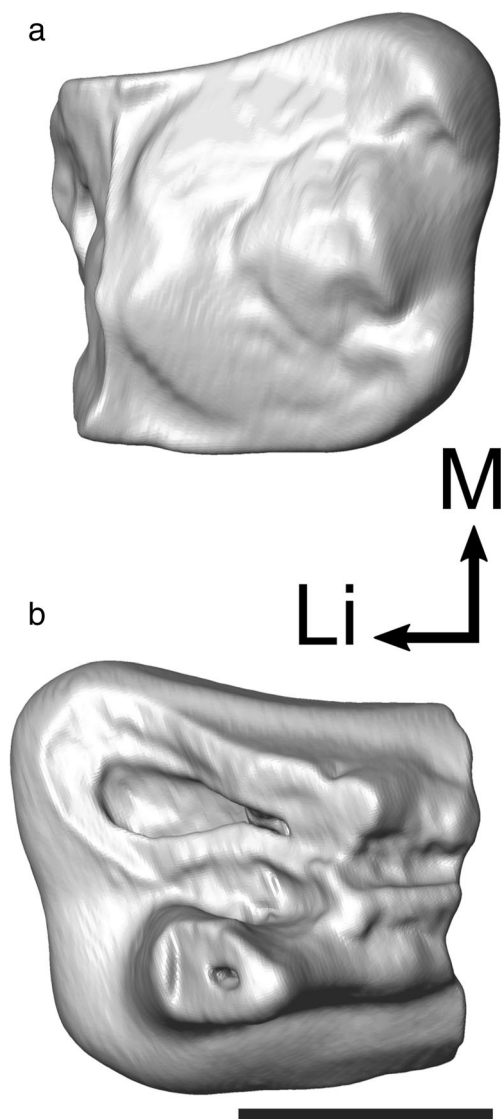


**Fig. 17** *Reigitherium* upper left third molar MPEF-PV 2369. **a** occlusal view; **b** dorsal view of roots. Mesial is towards the top of page. Scale bar is 1 mm and is for a and b. Directional arrows are for a only, Li - Lingual, M - Mesial

because of the large and laterally projecting form of the parastyle, a condition that matches the ultimate upper molar morphology in both *Peligrotherium* and *Coloniatherium*. The contrast in mediolateral width between the (damaged) base of the mesial root and base of the distal root is also greater than in the M2, suggesting that MPEF-PV 2369 succeeded this position. There is no trace of a lingual root in MPEF-PV 2369, possibly because of damage or its absence at this position.

The crown surface shows similar features to the M2, such as linear corrugations descending from the paracone, which are circumscribed by strong pre- and postparacristae. The paracristae themselves are labially terminated by a large parastyle and a smaller metastyle, respectively. Both of these styler cusps show frenular crests directed lingually towards the paracone. The stylocone also shows two crests running



mesially and distally towards the base of both of these stylar cusps, but lacks linear corrugations such as those present in the paracone. The M3 also lacks an ectostyle, unlike in the preceding two positions, and therefore has a steeper labial slope of the stylocone.

The mesial and distal roots are both damaged, but the shape of the compound interradicular crest and the roots' commencement from the cervical region are still clear. The mesial and distal roots are transversely wide at their base, and the lingual surface of these roots curves labially causing the roots to taper to a conical form underneath the stylar cusps. As in the preceding molar, a compound “Y” shaped interradicular crest can be seen between the mesial and distal roots. The two lateral branches of the interradicular crest are short, and both can be seen terminating into the mesial and distal root bases near the transverse midline of the tooth. A longer lingual branch of the compound interradicular crest runs towards the lingual edge of the fractured surface of MPEF-PV 2369. As mentioned above, it is not clear if there was a lingual root in this tooth position to form a lingual termination for the interradicular crest. The point of intersection of all three branches of the interradicular crest is located beneath the expression of the paracone on the crown surface.

## DISCUSSION

**Systematics of *Reigitherium*** The type specimen of *Reigitherium bunodontum* (MACN-RN-173; Bonaparte 1990) is a fragmentary isolated molar with all of its root structure and much of its crown detail effaced by postmortem processes. In its initial description Bonaparte (1990) insightfully recognized the mediolaterally widened crown structure seen in this specimen as indicative of the capacity for ectental occlusion (i.e., unilateral mastication with mediolateral translation) developed apomorphically in cladotherian mammals (Moore 1981; Kielan-Jaworowska et al. 2004). Thus, because of its advanced stem therian but non-tribosphenic characteristics the type specimen of *Reigitherium* was referred by Bonaparte (1990) to a monotypic family, probably related to Mesungulatidae, within the cladotherian lineage Dryolestoida. Additionally, the labial cusplids at the lateral end of the mesial and distal cingulids were inaccurately regarded as homologues of the anterior and posterior cingular cusps present along the lingual margins of the cingula in *Mesungulatum* (Bonaparte 1986; Rougier et al. 2009b), and it was this conflation that was ultimately responsible for the description of the type specimen as an upper left molar.

An additional complication in the interpretation of the type specimen is the crater-like excavation of the apex of the protoconid (“paracone” in Bonaparte 1990), possibly reflecting an accumulation of apical wear (Janis 1990) through

repeated puncture-crushing masticatory behaviors, or an exaggeration of it through postmortem erosion. Similar but less deeply excavated patterns of apical wear are also seen on the protoconids of first and second lower molar specimens from the La Colonia sample (MPEF-PV 2317 and MPEF-PV 2237). Interestingly, apical wear seen on the protoconid of the La Colonia m2 (MPEF-PV 2237) is shallower but more laterally extensive than in the Los Alamos holotype, stretching mesially onto the paracristid and with an additional apical pit on the apex of the metaconid.

The *Reigitherium* holotype also resembles the La Colonia m2 in unworn morphology, and most likely is attributable to this position. This was in effect posited by Pascual et al. (2000) by their suggestion that the holotype molar represented the next locus distal to the most posterior tooth preserved in their dentary specimen from the La Colonia Formation (MPEF-PV 606), and that at least one more tooth position must be placed distal to the holotype's locus. Surface data gathered from a cast of the *Reigitherium* holotype also support and qualify the identification of the Los Alamos specimen as a right lower m2. Compared to the m1 morphology seen in MPEF-PV 606, MPEF-PV 2317, MPEF-PV 2020, and MPEF-PV 2338, both MPEF-PV 2237 and the *Reigitherium* holotype show a medially inflected margin of the encainte distal to the protoconid. Additionally, the labial cusplid at the lateral end of the mesial cingulid is labially offset to a greater extent relative to the transverse position of the labial cusplid at the lateral end of the distal cingulid. Both of these cingular cusplids are also more closely appressed to the lateral aspect of the protoconid with concomitantly weaker development of their frenular crests. The lack of two labial cusplids near the lateral margin of the exodaenodont lobe in the holotype is most likely attributable to the fractured lateral surface of the specimen. Similarities between MACN-RN-173 and MPEF-PV 2337 are apparent and we feel confident in assigning the La Colonia material to the genus *Reigitherium*. Because of the limited extent of its hypodigm, however, there is no positive evidence for assigning the La Colonia material a conspecific status with *R. bunodontum* known from the (probably older) Los Alamos Formation, but we keep here the specific epithet until better material from the type locality allows evaluation of intraspecific variability in *Reigitherium*.

**Comparative Context** The presence of roughened, crenulated, or otherwise ornamented enamel in Mesozoic dental remains is seen almost exclusively in the non-therian mammaliaform clades Docodonta and Allotheria (including Multituberculata), in addition to several exceptional taxa such as *Brachyostrodon*. Among these taxa Butler (1997) pointed out that only the first three of these clades show a broadly oppositional relationship between the upper and lower dentitions. The additional presence in most docodont species of intermolar basins formed by the

flanks of adjacent molars provide strong reasons to suspect that any Mesozoic taxon showing this suite of traits should also be referable to Docodonts. This line of reasoning was presented and expanded on by Pascual et al. (2000) in their description of the first specimen of *Reigitherium* (MPEF-PV 606) from the La Colonia Formation, a dentary fragment with intact but worn p3-m1 (as in the newly recovered MPEF-PV 2338, Fig. 6). These authors rightly emphasized the presence of horizontal (apical) wear facets on the neomorphic cusplids as evidence for the presence of lingually extended upper molars, and characterize the protoconid as supporting mesially and distally directed crests. Additionally, what is referred to as the “main internal cingulum cusp” in Pascual et al. (2000) would correspond to cusp “c” under the schematic of docodont cusp homology provided by Butler (1997) and further elaborated by Luo and Martin (2007). Being the homolog of cusp “c,” this would make the metaconid in *Reigitherium* a correctly identified but renamed structure in Pascual et al. (2000). However, the majority of the subsequent argumentation provided by these authors for the docodont affinities of *Reigitherium* is the result of compounded misinterpretations based on the anatomy presented by the heavily worn specimen MPEF-PV 606 (Rougier and Apesteguía 2004; Rougier et al. 2011, 2012).

The highly molarized p4 of *Reigitherium* was interpreted by Pascual et al. (2000) as representing the first molar, and the Los Alamos type specimen, correctly identified as the locus succeeding the posterior tooth in MPEF-PV 606, was misinterpreted to be an m3. Because the *Reigitherium* type specimen does not show an “ultimate molar” morphology (e.g., a distally extended and tapering posterior crown) this was used by the authors as support for the presence of at least four molars in the dental formula in *Reigitherium*, matching the condition seen in many docodontans. The elongate p3 in *Reigitherium* was concomitantly interpreted to be a p4, and the inferred presence of a third lingual root at this position was used as another docodontan apomorphy. Further investigation of the p3 position in the expanded La Colonia sample described here (specimens MPEF-PV 2338, MPEF-PV 2372, and MPEF-PV 2376) using high resolution CT imaging does not corroborate the presence of a third lingual root at this position, or a small interradicular alveolus capable of accommodating this structure (although an accessory alveolus is present at the m1 position in MPEF-PV 2337). Observation of a neomorphic structure at the p3 position by Pascual et al. (2000) is likely attributable to the variable appearance of the interradicular crest, which likely forms a lingual extension with a similar appearance to the labial extension of the interradicular crest seen in the lower canine (MPEF-PV 2347, Fig. 9c). Finally, the crest of the encephalic as it crosses mesiodistally posterior to the protoconid was interpreted to represent the vestige of the “a-d crest” (or posteromedial crest of Sigogneau-Russell 2003), another feature diagnostic of docodonts. These initial misinterpretations provided inertia

for several hypotheses mentioned by Pascual et al. (2000) whereby the encephalic structure of *Reigitherium* was interpreted to be the product of a coalescence of several main cusplids (protoconid, paraconid, and “main internal cingulum cusp”/metaconid), cusplids (“posterior cingulum cusp,” “postero-internal cingulum cusp”) and lingual cingulid. The new lower molar specimens from La Colonia allow the identification of both the protoconid and metaconid as integral components of the encephalic; however, there is no evidence of any structure corresponding to the cusplids and lingual cingulid theorized by Pascual et al. (2000). Additionally, the continuous circuit of the lower molar encephalic mesial to the metaconid was not reconstructed in *Reigitherium* by these authors, but can be confirmed with the better preserved specimens now available. The hypothesized morphological evolution of the lower molars of *Reigitherium* by “expansion of area of opposition by expansion of lingual sector” (p 408) from a more typical docodont ancestor, and “shearing function between linear blades initiated in *Docodon* [that] was enhanced in *Reigitherium* by the enlargement of the occlusal surfaces of the molars, and its transformation, by thegosis, into flat blade-like facets” (p 405) are fundamental misstatements based on the above mentioned inaccurate but logically supported arguments. Naturally, our reinterpretation of the crown structure of *Reigitherium* also vitiates the hypothesized sister relationship between *Reigitherium* and *Docodon*.

Certainly, some of the newly discovered *Reigitherium* material does present morphological similarities to several docodont taxa, such as the presence of an angular notch on the ventral contour of the mandible. However, these similarities are much more easily explained as the result of convergence or retention of generalized features; the angular notch in particular is associated with the ventral deflection of the dentary’s angular process, either to accommodate a posterior facing angular articular facet in docodonts, or for muscular leverage in cladotherians (Kielan-Jaworowska et al. 2004).

Although the “pantotherian” similarities of docodonts, as originally mentioned by Simpson (1928, 1929), suggest that care should be taken in the taxonomic attribution of any new and apomorphic dental remains, the hypothesis of *Reigitherium* as the latest surviving and only known South American docodont has not been borne out by the weight of available evidence. However, later discoveries of Gondwanan docodonts from the early Middle Jurassic (Prasad and Manhas 2001, 2007) and near relatives from the Late Triassic (Datta 2005) have substantiated the suspicions of Pascual et al. (2000), and a preliminary report by Martin et al. (2013) suggested that docodonts may well have survived until the early Late Cretaceous of South America.

With the collection of these new and informative fossils the initial attribution of *Reigitherium* by Bonaparte (1990) to the South American radiation of dryolestoid mammals has once again become the most plausible phylogenetic hypothesis.

This taxonomic stance is not a default interpretation due to the abundance of meridiolestidan species and lack of ordinal diversity in the Cretaceous mammals of South America (Rougier et al. 2010). In fact, many of the same features suggestive of a docodontan relationship equally support a “eupantotherian” ancestry for *Reigitherium*. In particular, the bunodont and brachydont nature of the posterior cheek teeth point to a close relationship with the mesungulatoid meridiolestidans, an omnivorous-herbivorous radiation of rat-sized to dog-sized species found in Upper Cretaceous and Paleocene formations in Argentina (Bonaparte 1986; Rougier et al. 2009a and 2009b; Forasiepi et al. 2012) and Bolivia (Gayet et al. 2001). A series of explicit comparisons between *Reigitherium* and a sequence of taxa representative of increasingly more inclusive clades within Cladotheria (the advanced mesungulatoid *Peligrotherium*, dryolestoids, and the extant cladotherian groups Eutheria and Metatheria) will therefore provide a useful and appropriate context in which to interpret the evolutionary significance of *Reigitherium*.

**Comparison to *Peligrotherium*** Despite the enormous body mass differential between the shrew-sized *Reigitherium* and dog-sized *Peligrotherium*, there are several dental and gnathic features shared by both species suggestive of their exclusive relationship among the other South American cladotheres. These shared derived characteristics, as mentioned by Paez-Arango (2008) and Rougier et al. (2011, 2012), involve the elevation of occlusally functional cingulids, the acquisition of labial accessory cusps/cuspidules, and the inflated and intermittent condition of the primary trigon/trigonid crests.

This list of similarities can be validated and expanded based on evidence from the new La Colonia *Reigitherium* specimens described above, particularly with regard to the form of the dentary and upper dentition. Both taxa share the position of the posterior most mental foramen (the type specimen of *Peligrotherium* shows duplicate mental foramina on the right side only) posteroventral to the mesial root of the penultimate premolar. Additionally, the ventral contour of the dentary in both species reaches maximal convexity beneath the lower second molar. The upper molars also show a subrectangular to ovoid occlusal outline, with a complete loss of any kind of stylar lobes or projections.

While the apomorphies uniting *Reigitherium* and *Peligrotherium* are convincing, the morphological differences between these two species are also significant, and suggestive of the differing trajectories of trait evolution experienced by their lineages since their divergence from a more typical meridiolestidan common ancestor. These anatomical differences can be summarized by three major trends, possibly related to allometry and/or degree of herbivorous specialization: 1) the shortened and robust mandible of *Peligrotherium*, with its lateral deflection of the ascending ramus relative to the mandibular corpus; 2) the greater degree of molarization

(i.e., characteristics shared with true molars) of the upper penultimate and ultimate premolars in *Peligrotherium*, and greater degree of ultimate lower premolar molarization in *Reigitherium*; and 3) the greater development of the trigonid relative to cingulids and cuspidules in the lower molars of *Peligrotherium*, and greater development of the trigon relative to the mesial and distal cingula in the upper molars of *Reigitherium*.

Features associated with the strengthened mandible of *Peligrotherium* are the extensive symphysis, which reaches the level of the penultimate premolar (and which only reaches the level of p2 in *Reigitherium*), and reduced premolar dental formula with only three loci. The slight lateral deflection of the ascending ramus relative to the mandibular corpus creates a narrow and parallel tooth row, and is associated with a shallower anterior border of the masseteric fossa, and a coronoid process placed more laterally to the line of the lower molar alveoli.

The posterior upper premolars of *Reigitherium* show fewer similarities to the upper molars than in corresponding positions in *Peligrotherium*. This is evidenced by the more continuous cingula on the upper penultimate premolar of *Reigitherium* compared with the separated mesial and distal cingula on the true molars. Conversely, *Peligrotherium* shows greater posterior upper premolar molarization because of the shorter mesial and distal cingula on the distal two premolars and the presence of a lateral accessory cuspidule on the ultimate premolar (which does not form the labial terminus of either cingula). That being said, the distal two premolars of *Peligrotherium* do differ from the molar condition by consistently showing a wider distal cingulum relative to mesial cingulum, opposite to what is found in the true upper molars. The lower ultimate premolar of *Reigitherium* is actually more molarized relative to its counterpart in *Peligrotherium* because of its more labially extended mesial and distal cingulids, which are terminated labially by accessory cuspidules. In the lower ultimate premolar of *Peligrotherium* the labiolingual extent of the mesial and distal cingulids is narrower than the width of its trigonid region, and the size of this tooth position is also much greater than any of the true molars.

The lower molars of *Reigitherium* have departed from the plesiomorphic meridiolestidan condition to a greater degree than those of *Peligrotherium*, as shown by the almost complete loss of the paraconid (remaining as a small cuspidule only in the ultimate premolar), development of the encainte structure on all lower molars, relatively smaller size of the trigonid compared to the cingulids, and greater number and development of accessory cuspidules. Conversely, the upper molars of *Peligrotherium* have more elaborate marginal structures, based on the relatively smaller trigon relative to the greatly enlarged mesial and distal cingula. Additionally, the distally directed gradient of decreasing molar size in *Peligrotherium* is much steeper, causing the third upper molar to take on a

diminutive and sub-quadrate morphology. As mentioned above, it is unclear whether or not the structures identified here as paracristae in *Reigitherium* are actually vertically extended and lingually coalesced cingula. If this is indeed the case then the tall vertical extent of the upper molar cingula would be an additional apomorphic character uniting *Reigitherium* and *Peligrotherium*. However, under the interpretation followed here, the upper molars of *Reigitherium* are characterized by reduced cingula that are inconsequential for occlusion, opposite the condition seen in *Peligrotherium*. However, we feel this decision in the interpretation of the basic homologies of the upper molar is insufficiently supported. A definitive choice cannot be made without additional material or perhaps intermediate taxa filling the gaps between plesiomorphic mesungulatids and *Reigitherium*-like forms.

These differences between *Reigitherium* and *Peligrotherium* point to the diverging patterns of cheek tooth elaboration in these sister taxa. From an ancestral condition resembling *Coloniatherium*, the lower molariforms of *Reigitherium* have diverged to a greater degree and have widened considerably. Although the upper molars of both species are fairly derived, only in *Peligrotherium* is there an obvious tendency towards increased hypsodonty. Finally, probably the most apparent difference between *Reigitherium* and *Peligrotherium* is the intense but circumscribed crenulation of the primary trigon and encainte regions of all molariform cheek teeth in *Reigitherium*. This type of enamel ornamentation is not seen in *Peligrotherium* (or any other Cretaceous trechnotherian mammal). We hypothesize that this represents an adaptive response to selective pressures for increased herbivory unique to *Reigitherium* (outlined below).

**Comparison to Other Dryolestoids** Analyses of 44 dental and dentary characters among ten dryolestoid species support a nested position of *Reigitherium* among other South American endemic pre-tribosphenic mammals (see Fig. 18). The data are based on 38 characters described in Rougier et al. (2012) (updated based on the new *Reigitherium* sample), with six additional dental characters included. The character data and analysis specifications used here are available online in the supplementary materials associated with this report (Online Resource 2). Irrespective of optimality criterion, these results demonstrate that *Reigitherium* is best considered as a small and dentally sophisticated member of the Meridiolestida, and not a Late Cretaceous immigrant representative of a more basal mammaliaform lineage (as suggested by Pascual et al. 2000). These results corroborate the initial taxonomic assignment given by Bonaparte (1990), and further detailed by Bonaparte (1994), Bonaparte and Migale (2010), Rougier et al. (2011, 2012), and Wible and Rougier (2017).

Both Maximum Parsimony and Bayesian analyses treated all characters as equally weighted and unordered; however,

four of the included characters are parsimony uninformative (autapomorphic) and therefore were not considered in the Maximum Parsimony analysis.

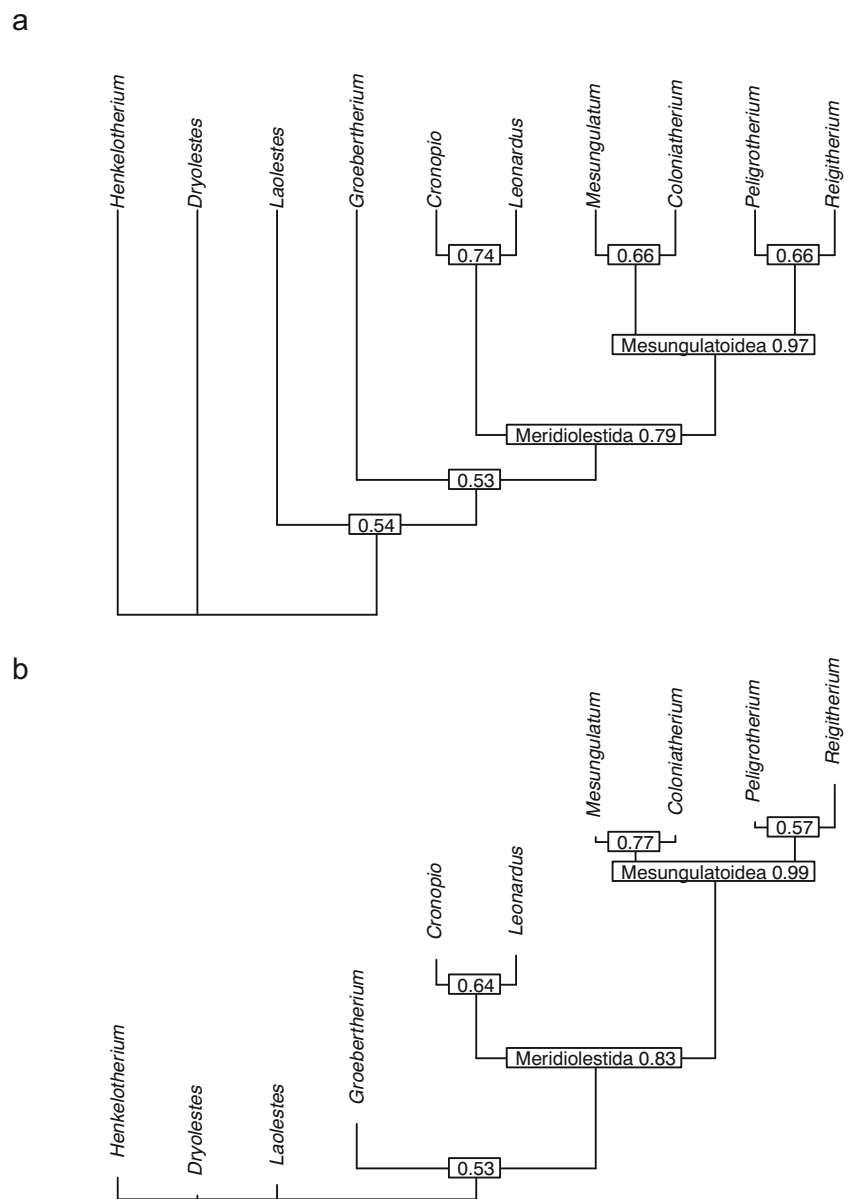
An exhaustive (branch and bound) Maximum Parsimony analysis, performed using PAUP\* version 4.0 (Swofford 2002), using these observations and assumptions, produced a single optimal topology with a length of 74 steps (Fig. 18a). This corresponds to a Consistency Index of 0.74 and Retention Index of 0.77. Randomization using ten thousand bootstrap replicates shows weak support for clades outside of Meridiolestida, particularly the node containing the North American *Laolestes* and all South American taxa. This provides only weak support for the dryolestoid relationships of the South American taxa, being supported by only one unambiguous synapomorphy (character 11, presence of a central crest in upper molariforms). Meridiolestidan relationships inter se are more reliably supported.

An uncalibrated Bayesian phylogenetic estimation based on the full 44 character matrix and a Mkv morphological likelihood model (Lewis 2001) integrated over gamma distributed rate variation produces the majority rule consensus and average branch lengths seen in Fig. 18b. These results are based on a Metropolis Coupled MCMC heuristic search implemented in the program MrBayes version 3.2 (Huelsenbeck and Ronquist 2001; Ronquist et al. 2012), using default parameters and a chain length of one million steps. Because the consensus topology produced does not resolve the exclusive relationship between *Laolestes* and the South American endemic clade, the dryolestoid affinities of the meridiolestidans are not supported. Aside from this polytomy at the root node, the topology and relative support values (posterior probabilities) within Meridiolestida correspond closely to the results found using Maximum Parsimony.

These results emphasize the apomorphic morphology diagnostic of Mesungulatoidea (which is well supported using either optimality criterion) discernable in *Reigitherium*. These characters include thickened enamel, tall cingulids, and mesiodistal compression of lower molar roots and the labial two upper molar roots. The trend towards increased bunodonty shown by mesungulatids and *Peligrotherium* is also apparent in *Reigitherium*, but is further accentuated by the localized crenulation seen only in this taxon. The presence of alveoli corresponding to three lower molar positions, and inferred matching presence of three upper molar positions, is also characteristic of Meridiolestida as a whole. The inferred presence of four premolar positions in *Reigitherium* is, however, disruptive to a completely parsimonious model of evolution for the premolar formula within Meridiolestida, as four premolars are also seen only in the plesiomorphic taxon *Cronopio*. Additionally, a Coniacian edentulous dentary fragment referred to Mesungulatoidea by Forasiepi et al. (2012) clearly preserves six postcanine tooth positions, most likely belonging to three premolars and three molars. The



**Fig. 18** Phylogeny of dryolestoid taxa and South American endemic cladotheres. **a** results of Maximum Parsimony analysis of 40 parsimony informative morphological characters, showing 50% majority rule consensus tree found using an exhaustive search. Node values are proportional support values found in 10 thousand bootstrap replicates. **b** majority rule consensus from Bayesian estimation using a Mkv morphological likelihood model. Branch lengths and node heights are estimated from posterior sample averages, and are not time-scaled. Posterior support values are shown at their respective nodes



homoplastic distribution of four premolar loci in both the most dentally plesiomorphic *Cronopio* and dentally derived *Reigitherium* suggests that a reduction to three premolars occurred in several separate lineages within Meridiolestida. However, for most meridiolestidans the dental formula cannot be accurately determined, and the optimization of this character may also be hindered because of the large amount of missing data.

Comparison with the dentition preserved in better known mesungulatooid taxa (See Figs. 1 and 2) suggests that the locus referred to as P1/p1 in *Reigitherium* contains the elements missing in the remaining species. The hypothesis that the first premolar in *Reigitherium* is a retained deciduous predecessor of the element referred to here as p2 is not supported by known aspects of the morphology of the anterior dentition

(i.e., simplified structure of the lower p1, without noticeably thinner enamel; Fig. 10). Conversely, the hypotheses that the p1 in *Reigitherium* could be a neomorphic acquisition, or that the element referred to as p2 in *Reigitherium* is actually a retained dp1 element can not be strictly ruled out, but are unlikely given the common modes of mammalian dental evolution and the relative size of the lower p2 (Luckett 1993). The appearance of a three-premolar mesungulatooid dental formula in the Coniacian therefore suggests that the lineage leading towards *Reigitherium* and *Peligrotherium* had split from the lineage leading to the Mesungulatoidea by at least the early Late Cretaceous.

As described by Crompton et al. (1994) and Wood and Rougier (2005), the enamel ultrastructure seen in the mesungulatooids *Mesungulatum* and *Coloniatherium* (referred

to as “La Colonia Dryolestoid” by the latter authors) also shows significant differences from the more derived pattern seen in *Reigitherium*. Specifically, the mesungulatid enamel contains a relatively large proportion of interprismatic, as opposed to prismatic, enamel crystallites. The distribution of enamel prisms and tubules is also highly polarized, with enamel tubules being restricted to the basal 25% of the total enamel thickness, and a consistently thick outer layer of aprismatic enamel near the outer enamel surface. In contrast, *Reigitherium* shows a complete loss of enamel seams, a regular and tightly packed distribution of enamel prisms nearly throughout the entire extent of its total enamel thickness, and a variably thick outer aprismatic layer near the outer enamel surface. This is a derived enamel microstructure pointing once again to the peculiar adaptation and long branch separating *Reigitherium* from other mesungulatoids. However, *Reigitherium* also displays several enamel ultrastructural synapomorphies with the mesungulatids and *Groebertherium*, such as the association of enamel tubules with the open side of enamel prism sheaths, and the orientation of interprismatic enamel crystallites perpendicular to the outer enamel surface, further supporting the meridiolestidan affinities of *Reigitherium*.

The mesiodistal compression of molar roots and the presence of a larger mesial root with a labially emarginated lateral aveolar border in the lower molars are also characters that have been suggested to represent a close affinity of the meridiolestidans as a whole with the holarctic Dryolestidae. However, the results of this summary analysis do not support the close relationship of these taxa to the exclusion of the more plesiomorphic paurodontid species *Henkelotherium* used as an outgroup. What has been reported about the enamel ultrastructure in *Laolestes* (Wood et al. 1999) and a Jurassic dryolestoid from Portugal (Lester and Koenigswald 1989) does support the possible derivation of the South American Mesozoic cladotheres from mammals of this type, and this is reflected in the phylogeny produced by Maximum Parsimony by the sister relationship of *Laolestes* with the South American endemic taxa. While the presence of incomplete enamel sheaths open toward the outer enamel surface, an abundance of interprismatic enamel material, and the presence of enamel seams are shared features seen in holarctic dryolestoids and the mesungulatids, they are also apparent in the enamel of *Spalacotheridium*, as reported by Wood et al. (1999). This leaves open a possible relationship of these South American endemic taxa with the spalacothere symmetrodonts, as suggested by Averianov et al. (2013). However, the presence of a prominent and posteroventrally deflected angular process is an apomorphic characteristic of cladotheres, which is apparent in several meridiolestidan taxa (*Cronopio*, *Peligrotherium*, and an unidentified mesungulatoid; Paez-Arango 2008; Rougier et al. 2011; Forasiepi et al. 2012; contra Averianov et al. 2013), which strongly supports a

cladotherian, if not dryolestidan, ancestry of Meridiolestida. The nested position of Meridiolestida and other South American taxa among the more typical dryolestoids is only recovered in our Maximum Parsimony phylogeny (Fig. 18), which therefore provides only weak support for the proposed relationship between these two groups. However, it is unlikely that the highly modified and limited material referable to *Reigitherium* will be able to definitively resolve the problem of the origin of the meridiolestidans as a whole. Better material of basal meridiolestidans and a focused phylogenetic analysis may be required to fully address this problem.

The relatively blunt cristids and thickened enamel along salient parts of the molar crowns in meridiolestidans, as compared to the dryolestid *Dryolestes*, is mentioned by Schultz and Martin (2011) as possible evidence for an alternative expression of the common utilization of the mesial and distal borders of the trigonid for masticatory grinding (sensu Kay and Hiimae 1974). Ostensibly, the deep downward sloping exposed dentine surfaces in worn molars of *Dryolestes* acted as receptacles for the oblique compression of food particles during rhythmic chewing. In Dryolestidae this function would be facilitated by the thinned enamel coating, which would accelerate abrasional wear and the formation of prevallid and postvallid compression zones. This is supported by the lack of attritional wear (pits and striations) characteristically found on surfaces experiencing tooth-tooth contact. If the founding lineage of South American endemic cladotheres was derived directly from dryolestids (or as our results suggest from a nearby sister lineage with enamel of more typical thickness) the trajectory seen in Meridiolestida towards morphological and enamel ultrastructural adaptation for a more routinely compressed trigonid can be detected at an incipient stage in the Late Jurassic in Holarctic dryolestoids. This hypothesis would also help explain the otherwise confusing fact that *Groebertherium*, while showing the most plesiomorphic lower molar morphology among South American cladotheres, has accumulated more synapomorphic enamel features (greater proportion of prismatic to interprismatic crystallites, and loss of enamel seams) than even the mesungulatid taxa *Mesungulatum* and *Coloniatherium*. By extension, the dentition of *Reigitherium* could also be seen as representing the most sophisticated product of this trend, with molars showing highly modified crown morphology and apomorphic enamel containing an abundance of regularly spaced prisms and a loss of enamel seams. Under the assumption that the amplification of compressive force is prerequisite for mammalian herbivory (Lucas 2004), the South American native cladotheres represent a greater expansion into the adaptive landscape of plant-based feeding than any northern symmetrodont, dryolestoid, or therian lineage in the Mesozoic.

**Comparison to Northern Tribosphenic Mammals** The presence of a cingular protocone in the upper dentition has been

heralded as one of the most consequential anatomical developments in the therian lineage (Patterson 1956; Crompton 1971; Crompton and Kielan-Jaworowska 1978; Davis 2011). The defining characteristic of this transformation is a shift from a bi-directionally convex lingual cingulum on upper molars (as seen in *Peramus*; Mills 1964; Davis 2012) into a radially convex lingual protocone (as seen in *Kielantherium*; Lopatin and Averianov 2007). The co-option of this feature has allowed for many Cenozoic tribosphenic mammals to specialize their posterior dentitions toward highly efficient “grinding” (sensu Rensberger 1973) types of mastication (Crompton 1971; Davis 2012). However, the functional importance of the protocone at the time of its first occurrence among aegialodontids and therians (the northern tribosphenic clade) is difficult to interpret. This is because of the apparent lack of increased abundance or diversity in northern tribosphenic fossils near their probable origin during the Late Jurassic; and also because of the manifest capacity of pre-tribosphenic stem

therian lineages to develop complex and bunodont crown morphologies, without the benefit of a protocone or a basined talonid. This capacity for elaborate mastication in pre-tribosphenic stem therians is nowhere better demonstrated than in *Reigitherium* and the other mesungulatoid meridiolestidans, making these species an appropriate comparative sample with which to contrast the trajectory of tribosphenic and pseudotribosphenic cheek-tooth specialization.

While gestalt similarities of the molar morphology seen in mesungulatoids and omnivorous Paleogene therians have been noted by several authors (Bonaparte 1986; Paez-Arango 2008), the common assumption that the attainment of tribospheny presents a morphological gap too large to cross with traditional distance-based or landmark-based morphometric methods has precluded any formal quantitative comparison of pre-tribosphenic and tribosphenic taxa. However, the recent development of “homology-free” dental metrics based on high-level features of crown topography provides

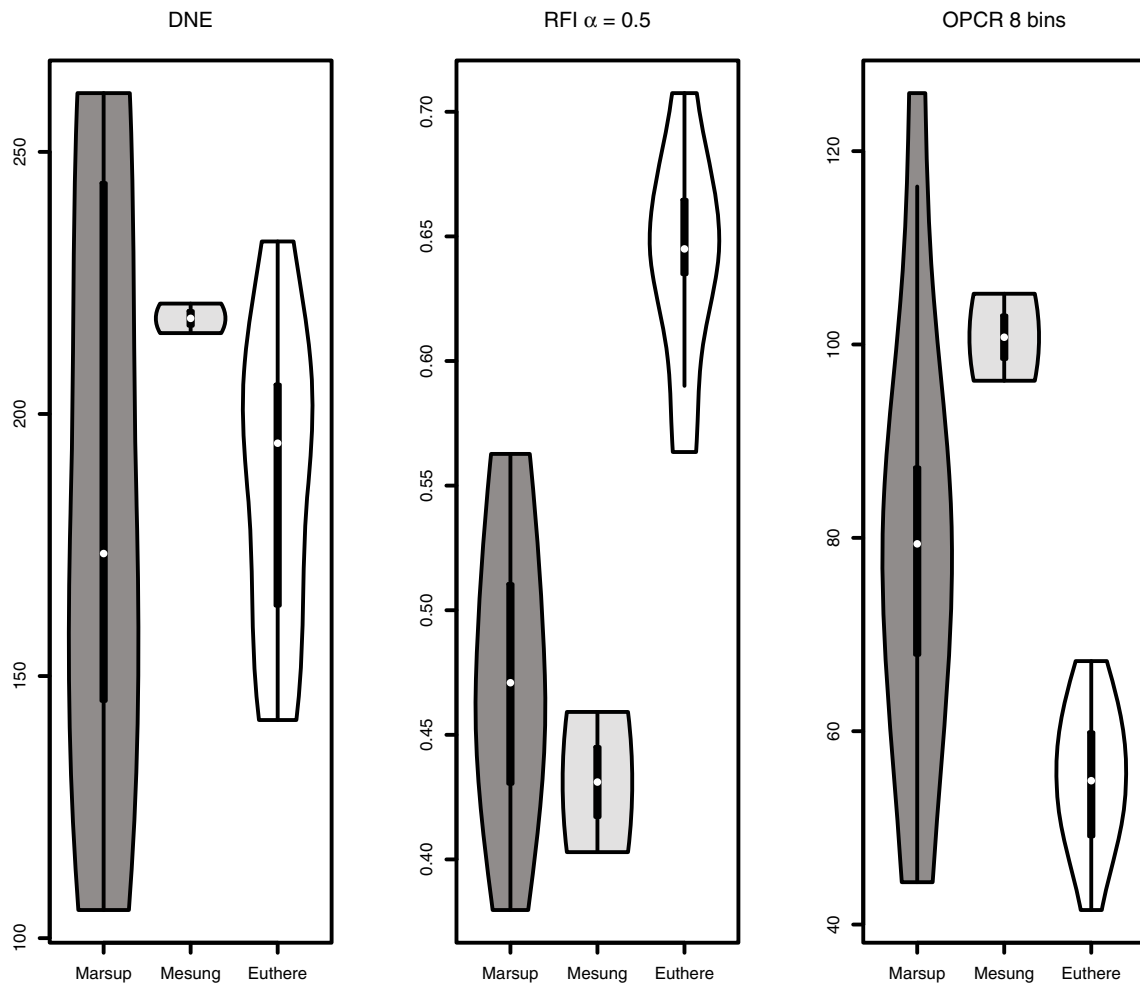


**Fig. 19** Violin plots showing distribution of dental topographic values for marsupials ( $N = 8$ ), mesungulatoids ( $N = 2$ ), and eutherians ( $N = 13$ ), respectively. White circles show median values, black bars delimit lower 25th and 75th percentiles, and shaded boxes encompass full data range. This sample demonstrates the broad overlap of all taxa in DNE.

Additionally, the significant differences in RFI and OPCR between the advanced mesungulatoids and marsupials on the one hand, and Cretaceous eutherians on the other, are also apparent. The mesungulatoid and marsupial groups do not significantly differ in any of the dental topography metrics analyzed

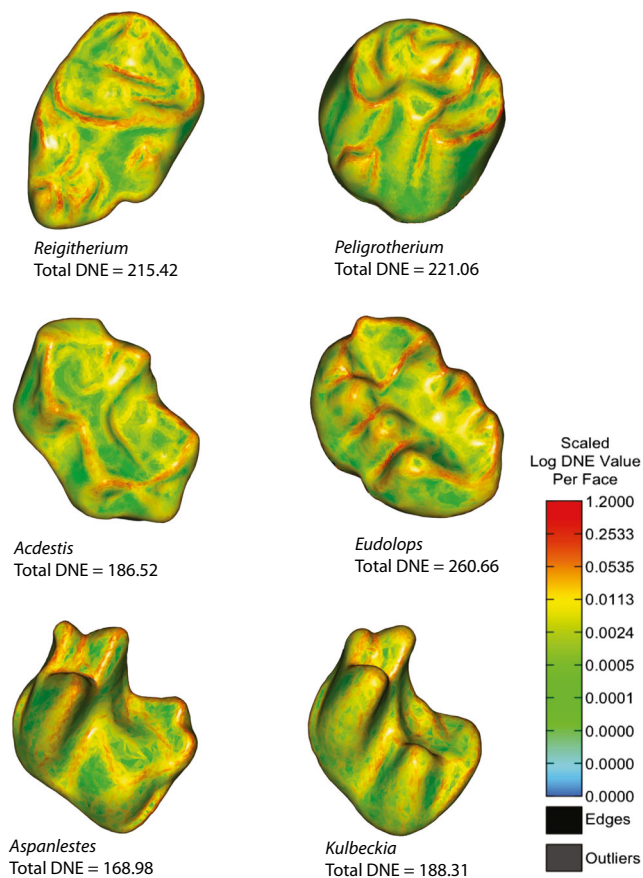


**Fig. 20** Comparison of Dirichlet Normal Energy values in representative lower left second molars in oblique view. Mesial is toward the top left, and lingual is towards the top right of the page

an opportunity to compare functionally interpretable aspects of tooth shape across a wide variety of extinct and extant taxa (e.g., Wilson et al. 2012). As the acquisition of the tribosphenic condition is predicated on the punctuational appearance of a neomorphic feature of the upper dentition (the protocone), the analysis here is limited to the morphology of the lower second molar. As the lower molars of stem therians show a more continuous pattern of shape change across the pre-tribosphenic/tribosphenic phylogenetic boundary, quantitative comparisons of lower molar shape are more likely to produce a continuous (as opposed to disjoint) distribution of measured dental topography metric values. As noted above, the three most popular dental topography metrics (Orientation Patch Count, OPC/OPCR; Relief Index, RFI; and Dirichlet Normal Energy, DNE) have been given a common implementation with the R package *Molar* (Pampush et al. 2016), which is used in the Dental Topography Analysis reported below (see materials and methods).

These metrics have functional interpretations based on analogy to simple percussive tools. The value of OPCR can be analogized with the number of tools on a tooth's surface. Similarly, DNE can be thought of as the sharpness of the average tool, and RFI the average tool's height. Under this

interpretation, the trend toward increased herbivory in tribosphenic mammals is represented by the increase in number of shorter tools on the lower second molar surface (as seen in Figs. 19, 20 and 21).

Small-bodied marsupials are the tribosphenic mammals thought to competitively replace the latest Cretaceous mesungulatooids, particularly species within Paucituberculata and Polydolopimorphia (Goin et al. 2016). The earliest evidence for the radiation of these major subgroups of small-bodied marsupials is seen in the Cretaceous or Paleocene Peruvian Chulpas locality (Sigé et al. 2004). They are, however, not found anywhere in sympatric association with meridiolestidan taxa.

The  $N = 8$  marsupial specimens analyzed in this report are the early didelphimorph *Caroloameghinia*, polydolopimorphians *Roberthoffstetteria* (a Paleocene sillustaniid), *Epidolops ameghenoi* (a bonapartheriid), and the polydolopids *Polydolops rothi*, *Polydolops thomasi*, and *Eudolops tetragonus* (= *Eudolops caroliameghinoi*); the early Miocene caenolestoids analyzed include *Acdestis owenii* and *Palaeotheres lemoinei* (both palaeotheres) (Goin et al. 2016). These species show a range of trigonid and talonid morphologies that are highly modified compared to the plesiomorphic tribosphenic condition and, therefore, represent the most herbivorously adapted marsupials in the early Cenozoic of South America.

As a counterpoint to the extreme dental specialization seen in the South American mesungulatooids and marsupials,  $N = 13$  stem eutherian specimens are analyzed as well. These taxa

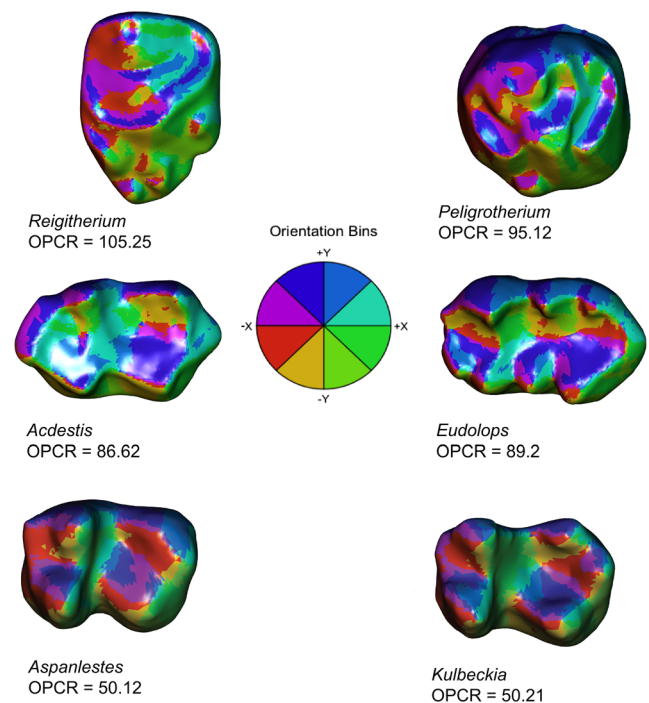


**Fig. 21** Comparison of Orientation Patch Count values in representative lower left second molars. Mesial is toward the left, and lingual is towards the top of the page



are Turonian (94–90 mya) stem eutherians, outside of the placental crown group, which have been recovered from the Bissekty Formation of western Uzbekistan (Archibald and Averianov 2003, 2012). The Bissekty Fauna represents the first fossil environment with a mammalian component dominated by eutherians (nine out of 12 species), and the two families studied for this analysis (zhelestids and zalambdalestids) represent the most herbivorously adapted tribosphenic taxa, not only in their fauna but also the entire Mesozoic until the latest Cretaceous. The zhelestids included in this project, in successively increasing body size, are *Aspanlestes aptap*, *Zhelestes temirkazyk*, *Eoungulatum* sp., and *Parazhelestes* sp. These taxa have low crowned, basally inflated lower molars, with well-developed talonid attritional wear surfaces, but they are still fairly close morphologically to the primitive therian condition. The only zalambdalestid taxon analyzed here is *Kulbeckia* sp., which, being the most primitive member of the Zalambdalestidae, has a lower trigonid relative to the talonid, compared to later members of this family.

When the topographic metrics described above are applied to the lower second molars of stem eutherians, marsupials, *Reigitherium*, and *Peligrotherium*, it is clear that the pre-tribosphenic mesungulatooid taxa lie broadly within the range of values seen in both Cretaceous and Paleogene therians. Separate one-way ANOVAs, implemented using base functions in the R programming language with taxonomic category (eutherian, marsupial, or mesungulatooid) as a predictor and OPCR, RFI, and DNE as responses, further clarify the variation in dental topography between these taxa. The data used for these analyses are available in the supplementary materials associated with this report (Online Resource 1).

The insignificant ( $p = 0.608$ ) result of the ANOVA with DNE as a response suggests that there is no systematic differentiation of molar sharpness between tribosphenic and pre-tribosphenic taxa, or between Cretaceous and Paleogene forms. This is surprising given the stereotypically insectivorous feeding strategy often assumed for Cretaceous eutherian taxa. However, this lack of significance may be attributed to the small sample sizes involved, and/or to the attainment of a degree of omnivory by all taxa considered, even the Cretaceous zhelestids and zalmbdalestids (see Fig. 20).

Both one-way ANOVA and Kruskal-Wallis omnibus tests of OPCR and RFI show that there are significant differences between the major clades considered. For each of these two dental topographic variables, three 2-sample T-tests (unadjusted for multiple comparisons) were subsequently used as post hoc tests to define the differentiation detected by each omnibus test (non-parametric post hoc Mann-Whitney-Wilcoxon tests show identical patterns of significance). For both OPCR and RFI, post hoc analysis suggests that no significant differences exist between the South American marsupials and mesungulatooids (*Reigitherium* and *Peligrotherium*).

However, the OPCR and RFI for the South American mammals are significantly differentiated (OPCR higher and RFI lower, on average) from the corresponding metrics in the Cretaceous eutherians (see Fig. 21). Among the sampled marsupials OPCR in palaeothentids and the polydolopid *Eudolops* are closest to the advanced mesungulatooids. Interestingly members of these families are inferred by Goin et al. (2016: chapter 6) as being mixed feeders of high energy food products, with palaeothentids representing “insectivorous-frugivorous” and polydolopids representing “frugivorous-insectivorous” feeding strategies, respectively. The surprising fact that the bonapartheriid *Epidolops* and *Polydolops rothi* are closest in OPCR to stem eutherians is likely a byproduct of the advanced stage of premortem dental wear seen in these cast specimens. These taxa also show the lowest DNE values among the South American forms. Additionally, the plesiomorphic silustaniid polydolopiform *Roberthoffstetteria* and the “primate-like” didelphimorph *Caroloameghinia* both show values of OPCR and RFI intermediate to the sampled eutherians and mesungulatooids. This finding makes sense given the early-diverging phylogenetic and stratigraphic positions (from the early Paleocene and early Eocene, respectively) of these species, and suggests that they attained an incipient form of herbivory which is further developed in later marsupial groups. The caroloameghiniids are also estimated to be mixed “insectivorous-frugivorous” feeders by Goin et al. (2016).

These results demonstrate that the trends in dental topography seen across the K-Pg boundary in omnivorous therians, namely an increase in complexity and decrease in relative crown height, are seen precociously in the Cretaceous and early Paleocene South American taxa *Reigitherium* and *Peligrotherium*.

The crenulation of the trigonid in *Reigitherium* (and extensive cingulids seen in *Peligrotherium*) can be seen as an alternative approach to increasing OPCR without the aid of a well-developed talonid, like those present in therians. Conversely, the mortar-and-pestle protocone-and-talonid relationship can therefore be considered just one more tool, or one more set of tools, in the tuberculosectorial molar. This points to the advanced degree of herbivory attained by the mesungulatooids, possibly in response to the earlier availability of angiosperm reproductive structures in gondwanan floras (Wilf et al. 2013; Goin et al. 2016). Alternatively, the acquisition of the protocone and the talonid grinding surface can be considered a relatively minor morphological modification, with the later convergent development of a hypocone in many tribosphenic lineages representing the adaptive breakthrough responsible for the modern success of many groups of therian mammals (Hunter and Jernvall 1995).

Regardless of how significant the early development of the protocone was to the first tribosphenidans, the fact that a major

clade of pre-tribosphenic mammals can occupy a more herbivorous niche along the spectrum of omnivory-herbivory defined by a sample of tribosphenic mammals suggests that functional demands constrained the morphology of both types of molars in a similar fashion. This undermines explanations positing molar formula and morphology as unique determining factors for the Cenozoic adaptive radiation of therian mammals.

## Conclusion

Aside from several Paleogene experiments such as *Bemalambda* and *Arsinoitherium* (Rose 2006), no therian clade has successfully adapted towards obligate herbivory with a reduced or absent protocone. This, combined with the presumed insectivory of Mesozoic stem therians, resulted in *Reigitherium* being overlooked as one of the first and most overt examples of ecological expansion into a plant-based feeding strategy (along with multituberculates and gondwanatheres). The new material presented here provides additional evidence of the uniquely derived and complex dentition developed in the genus *Reigitherium*, and summarizes the best current hypotheses for its phylogenetic location and feeding strategy. The newly described upper dentition provides abundant support for the pre-tribosphenic position of *Reigitherium* within the larger radiation of endemic South American cladotheres. Additionally, high-level analysis of the lower second molar demonstrates the advanced stage of herbivory attained by this taxon and its closest meridiolestidan relatives.

While the derived morphology of *Reigitherium* contributes little additional resolution on relationships of Meridiolestida among basal stem therians, the summary phylogenies reported here support the sister relationship of *Reigitherium* with the most derived meridiolestidans such as *Peligrotherium*, and the mesungulatids. Each member of this advanced mesungulatoid clade shows many dental characteristics traditionally associated with omnivory and herbivory in extant mammals, such as bunodonty, hypsodonty, exodaenodonty, neomorphic cusps/cuspidids, enlarged cingula/cingulids, deepening and connation of molar roots, molarization of premolars, and with *Reigitherium* enamel ornamentation. This is an impressive roster of apomorphies for any herbivorous mammalian group, and the fact that these traits make their earliest appearance in the South American Cretaceous points toward a glaring deficit in the current narrative of the radiation of mammals near the K-Pg boundary. The Upper Cretaceous of South America offers a systematic and morphological landscape distinct from the benchmark communities of North America and Asia; and as such sets up a natural experiment of the influence of global trends (climate, floral expansion, etc.) on faunas with radically different heritage.

**Acknowledgments** We would like to thank Dr. Rubén Cúneo, Leandro Canessa, and other personnel of the Museo Paleontológico Egidio Feruglio, Chubut, Argentina for years of support. We are additionally grateful to David Archibald and Ken Rose for their deep insight into mammalian evolution and access to the therian comparative specimens used here, and Patrick Luckett for helpful comments on dental homology and proofreading early drafts of the manuscript. Tim Phelps and the other faculty at Johns Hopkins University Department of Art as Applied to Medicine provided expert input and guidance to TH in the production of illustrations, and Justin Gladman and Doug Boyer at Duke University's Shared Materials and Instrumentation Facility (SMIF) graciously contributed access and assistance with the high quality imaging required for the description of small enigmatic mammalian fossils, for which we are also very grateful. We would also like to thank Dr. Alejandro Karmaraz for access to the collections of Museo Argentino de Ciencias Naturales, Buenos Aires, Argentina, and intellectual and material support through the years. Finally, we thank Rosío B. Vera for her diligent assistance in picking through La Colonia sediments. This research was supported by NSF via the DEB 0946430 and DEB 1068089 grants (to GWR), USA, and by the RAICES program (PICT-2016-3682), Agencia de Investigación Científica, CONICET, Argentina.

## References

- Andreis RR (1987) The Late Cretaceous fauna of Los Alamitos, Patagonia Argentina. I. Stratigraphy and paleoenvironments. *Revista del Museo Argentino de Ciencias Naturales Bernardino Rivadavia* 3:103–110
- Andreis RR, Bense CA, Rial G (1989) La transgresión marina del Cretácico Tardío en el borde SE de la Meseta de Somuncurá, Río Negro, Patagonia Septentrional, Argentina. In: *Contribuciones de los Simposios sobre el Cretácico de América Latina, Parte A: Eventos y Registros Sedimentarios*, pp 165–194
- Archibald JD, Deutschman DH (2001) Quantitative analysis of the timing of the origin and diversification of extant placental orders. *J Mammal Evol* 8:107–124
- Archibald JD, Averianov AO (2003) The Late Cretaceous placental mammal *Kulbeckia*. *J Vertebr Paleontol* 23:404–419
- Archibald JD, Averianov AO (2012) Phylogenetic analysis, taxonomic revision, and dental ontogeny of the Cretaceous Zhelestidae (Mammalia: Eutheria). *Zool Linn Soc* 164:361–426
- Ardolino A, Delpino D (1987) Senoniano (continental-marino) Comarca Nordpatagónica, Provincia del Chubut, Argentina. *X Congreso Geológico Argentino (Tucumán) Actas* 3: 193–196
- Ardolino A, Franchi M (1996) Hoja geológica 4366 - I Telsen. Provincia del Chubut. Programa Nacional de Cartas Geológicas de la República Argentina, escala 1:250.000. Dirección Nacional del Servicio Geológico, Buenos Aires, Boletín 215, 110 pp
- Averianov AO, Martin T, Lopatin AV (2013) A new phylogeny for the basal Trechnotheria and Cladotheria and affinities of the South American endemic Late Cretaceous mammals. *Naturwissenschaften* 100:311–326
- Bonaparte JF (1986) Sobre *Mesungulatum houssayi* y nuevos mamíferos Cretácicos de Patagonia, Argentina. *Actas IV Congreso Argentino de Paleontología y Bioestratigrafía* 2:48–61
- Bonaparte J (1990) New Late Cretaceous mammals from the Los Alamitos Formation, northern Patagonia. *Geogr Res* 6:63–93
- Bonaparte JF (1994) Approach to the significance of the Late Cretaceous mammals of South America. *Berliner geowissenschaft Abh* 13:1–44
- Bonaparte JF, Migale LA (2010) Protomamíferos y Mamíferos Mesozoicos de América del Sur. Museo de Ciencias Naturales Carlos Ameghino, Buenos Aires

- Bonaparte JF, Van Valen LM, Kramartz A (1993) La fauna local de Punta Peligro, Paleoceno inferior, de la Provincia del Chubut, Patagonia, Argentina. *Evol Monogr* 14:1–61
- Boyer DM (2008) Relief index of second mandibular molars is a correlate of diet among prosimian primates and other euarchontan mammals. *J Hum Evol* 55:1118–1137.
- Bunn JM, Boyer DM, Lipman Y, St Clair EM, Jernvall J, Daubechies I (2011) Comparing Dirichlet normal surface energy of tooth crowns, a new technique of molar shape quantification for dietary inference, with previous methods in isolation and in combination. *Am J Phys Anthropol* 145:247–261
- Butler PM (1939) Studies of the mammalian dentition—differentiation of the post-canine dentition. *J Zool* 109:1–36
- Butler PM (1948) On the evolution of the skull and teeth in the Erinaceidae, with special reference to fossil material in the British Museum. *J Zool* 118:446–500
- Butler PM (1997) An alternative hypothesis on the origin of docodont molar teeth. *J Vertebr Paleontol* 17:435–439
- Cúneo NR, Gandolfo MA, Zamalao MC, Hermsen E (2014) Late Cretaceous Aquatic Plant World in Patagonia, Argentina. *PLoS One* 9:1–18
- Crompton AW (1971) The origin of the tribosphenic molar. In: Kermack DM, Kermack, KA (eds) *Early Mammals*. *Zool J Linn Soc* 50: 65–87
- Crompton AW, Kielan-Jaworowska Z (1978) Molar structure and occlusion in Cretaceous therian mammals. In: Butler PM, Joysey KA (eds) *Development, Function and Evolution of Teeth*. Academic Press, London, pp 249–287
- Crompton AW, CB Wood, Stern DN (1994) Differential wear of enamel: a mechanism for maintaining sharp cutting edges. In: Bels VL, Chardon M, Vandewalle P (eds) *Biomechanics of Feeding in Vertebrates*. Springer, Berlin, pp 321–346
- Datta PM (2005) Earliest mammal with transversely expanded upper molar from the Late Triassic (Carnian) Tiki Formation, South Rewa Gondwana Basin, India. *J Vertebr Paleontol* 25:200–207
- Davis BM (2011) Evolution of the tribosphenic molar pattern in early mammals, with comments on the “dual-origin” hypothesis. *J Mammal Evol* 18:227–244
- Davis BM (2012) Micro-computed tomography reveals a diversity of Peramuran mammals from the Purbeck Group (Berriasian) of England. *Palaeontology* 55:789–817
- Drummond AJ, Bouckaert RR (2015) *Bayesian Evolutionary Analysis with BEAST*. Cambridge University Press, Cambridge
- Evans AR, Wilson GP, Fortelius M, Jernvall J (2007) High-level similarity of dentitions in carnivorous and rodents. *Nature* 445:78–81
- Forasiepi AM, Coria RA, Hurum J, Currie PJ (2012) First dryolestoid (Mammalia, Dryolestoidea, Meridiolestida) from the Coniacian of Patagonia and new evidence on their early radiation in South America. *Ameghiniana* 49:497–504
- Gasparini Z, Sterli J, Parras A, O’Gorman JP, Salgado L, Varela J, Pol D (2015) Late Cretaceous reptilian biota of the La Colonia Formation, Central Patagonia, Argentina: occurrences, preservation and paleoenvironments. *Cret Res* 54:154–168
- Gayet M, Marshall LG, Sempere T, Meunier FJ, Cappetta H, Rage JC (2001). Middle Maastrichtian vertebrates (fishes, amphibians, dinosaurs and other reptiles, mammals) from Pajcha Pata (Bolivia). Biostratigraphic, palaeoecologic and palaeobiogeographic implications. *Palaeogeogr Palaeoclimatol Palaeoecol* 169:39–68
- Gelfo JN, Pascual R (2001) *Peligrotherium tropicalis* (Mammalia, Dryolestida) from the early Paleocene of Patagonia, a survival from a Mesozoic Gondwanan radiation. *Geodiversitas* 23:369–379
- Goin FJ, Woodburne MO, Zimicz AN, Martin GM, Chornogubsky L (2016) *A Brief History of South American Metatherians*. Springer, Heidelberg
- Gould SJ (2002) *The Structure of Evolutionary Theory*. Harvard University Press, Cambridge
- Guler MV, Borel CM, Brinkhuis H, Navarro E, Astini R (2014) Brackish to freshwater dinoflagellate cyst assemblages from the La Colonia Formation (Paleocene?), northeastern Patagonia, Argentina. *Ameghiniana* 51:141–153
- Grossnickle DM, Polly PD (2013) Mammal disparity decreases during the Cretaceous angiosperm radiation. *Proc R Soc Lond B* 280: 20132110
- Grossnickle DM, Newham E (2016). Therian mammals experience an ecomorphological radiation during the Late Cretaceous and selective extinction at the K–Pg boundary. *Proc R Soc Lond B* 283: 20160256
- Halliday TJD, Goswami A (2016) Eutherian morphological disparity across the end-Cretaceous mass extinction. *Biol J Linn Soc* 118: 152–168
- Hershkovitz P (1971) Basic crown patterns and cusp homologies of mammalian teeth. In: Dahlberg AA (ed) *Dental Morphology and Evolution*. University of Chicago Press, Chicago, pp 95–150
- Huelsenbeck JP, Ronquist F (2001) MRBAYES: Bayesian inference of phylogeny. *Bioinformatics* 17:754–755
- Hugo CA, Leanza HA (2001) Hoja geológica 3969-IV, general roca. Provincias de Río Negro y Neuquén. Boletín Servicio Geológico Minero Argentino, Instituto de Geología y Recursos Minerales 308:1–65
- Hunter JP, Jernvall J (1995) The hypocone as a key innovation in mammalian evolution. *Proc Natl Acad Sci USA* 92:10718–10722
- Janis CM (1990) The correlation between diet and dental wear in herbivorous mammals, and its relationship to the determination of diets of extinct species. In: Boucot AJ (ed) *Paleobiological Evidence for Rates of Coevolution and Behavioral Evolution*. Elsevier, New York, pp 241–259
- Jernvall J, Hunter JP, Fortelius M (1996) Molar tooth diversity, disparity, and ecology in Cenozoic ungulate radiations. *Science* 274:1489–1492
- Kay RF, Hiiemae KM (1974) Jaw movement and tooth use in recent and fossil primates. *Am J Phys Anthropol* 40:227–256
- Kielan-Jaworowska Z, Cifelli RL, Luo ZX (2004) *Mammals from the Age of Dinosaurs: Origins, Evolution, and Structure*. Columbia University Press, New York
- Lester KS, Koenigswald W von (1989) Crystallite orientation discontinuities and the evolution of mammalian enamel—or, when is a prism? *Scanning microscopy* 3:645–662
- Lewis PO (2001) A likelihood approach to estimating phylogeny from discrete morphological character data. *Syst Biol* 50:913–925
- Lopatin A, Averianov AO (2007) *Kielantherium*, a basal tribosphenic mammal from the Early Cretaceous of Mongolia, with new data on the aegialodontian dentition. *Acta Palaeontol Pol* 52:441–446
- Lucas PW (2004) *Dental Functional Morphology: How Teeth Work*. Cambridge University Press, Cambridge
- Luckett WP (1993) An ontogenetic assessment of dental homologies in therian mammals. In: Szalay FS, Novacek MJ, McKenna MC (eds) *Mammal Phylogeny: Mesozoic Differentiation, Multituberculates, Monotremes, Early Therians, and Marsupials*. Springer, New York, pp 182–204
- Luo ZX, Martin T (2007) Analysis of molar structure and phylogeny of docodont genera. *Bull Carnegie Mus Nat Hist* 39:27–47
- Malumíán N, Caramés A (1995) El Daniano marino de Patagonia (Argentina): Paleobiogeografía de los foraminíferos bentónicos. In: Nández C (ed) *Paleógeno de América del Sur*. Asociación Paleontológica Argentina, Publicación Especial 3, Buenos Aires, pp 83–105
- Martin T, Goin, F, Chornogubsky L, Gelfo J, Shultz J (2013) Early Late Cretaceous (Cenomanian) mammals and other vertebrates from the Mata Amarilla Formation of southern Patagonia (Argentina). *Soc Vertebr Paleontol Annual Meeting Abstracts*
- McDowell SB (1958) The Greater Antillean insectivores. *Bull Am Mus Nat Hist* 115:113–214



- McKenna MC (1975) Toward a phylogenetic classification of the Mammalia. In: Lockett, WP, Szalay FS (eds) *Phylogeny of the Primates*. Plenum Press, New York, pp 21–46
- Mills JRE (1964) The dentitions of *Peramus* and *Amphitherium*. *Proc Linn Soc Lond* 175:117–133
- Moore WJ (1981) *The Mammalian Skull*. Cambridge University Press, Cambridge
- O’Gorman JP, Salgado L, Varela J, Parras A (2013) Elasmosaurs (Sauropterygia, Plesiosauria) from La Colonia Formation (Campanian-Maastrichtian), Argentina. *Alcheringa* 37:259–267
- Paez-Arango N (2008) Dental and craniomandibular anatomy of *Peligrotherium tropicalis*: the evolutionary radiation of South American dryolestoid mammals. Dissertation, University of Louisville
- Page R, Ardolino A, de Barrio RE, Franchi M, Lizuain A, Page S, Silva Nieto D (1999) Estratigrafía del Jurásico y Cretácico del Macizo de Somún Curá, provincias de Río Negro y Chubut. In: Caminos R (ed) *Geología Argentina*. Servicio Geológico Minero Argentino SEGEMAR Anales 29, Buenos Aires, pp 460–488
- Pampush JD, Winchester JM, Morse PE, Vining AQ, Boyer DM, Kay RF (2016) Introducing molaR: a new R package for quantitative topographic analysis of teeth (and other topographic surfaces). *J Mammal Evol* 23:397–412
- Pascual R, Goin FJ, González P, Ardolino A, Puerta PF (2000) A highly derived docodont from the Patagonian Late Cretaceous: evolutionary implications for Gondwanan mammals. *Geodiversitas* 22:395–414
- Patterson B (1956) Early Cretaceous mammals and the evolution of mammalian molar teeth. *Fieldiana Geol* 13:1–105
- Pesce AH (1979) Estratigrafía del arroyo Perdido en su tramo medio e inferior provincia del Chubut. VII Congreso Geológico Argentino (Neuquén, 1978), *Actas* 1:315–333
- Prasad GVR, Manhas BK (2001) First docodont mammals of Laurasian affinities from India. *Curr Sci* 81:1235–1238
- Prasad, GVR, Manhas BK (2007) A new docodont mammal from the Jurassic Kota Formation of India. *Palaeontol Electronica* 11:1–11
- Prothero DR (1981) New Jurassic mammals from Como Bluff, Wyoming, and the interrelationships of non-tribosphenic Theria. *Bull Am Mus Nat Hist* 167:277–326
- Rensberger JM (1973) An occlusal model for mastication and dental wear in herbivorous mammals. *J Paleontol* 47:515–528
- Riccardi AC (1987) Cretaceous paleogeography of southern South America. *Palaeogeogr Palaeoclimatol Palaeoecol* 59:169–195
- Ronquist F, Teslenko M, van der Mark P, Ayres D, Darling A, Höhna S, Larget B, Liu L, Suchard MA, Huelsenbeck JP (2012) MrBayes 3.2: efficient Bayesian phylogenetic inference and model choice across a large model space. *Syst Biol* 61:539–542
- Rose KD (2006) *The Beginning of the Age of Mammals*. Johns Hopkins University Press, Baltimore
- Rougier GW, S Apesteeguía (2004) The Mesozoic radiation of dryolestoids in South America: dental and cranial evidence. *J Vertebr Paleontol* 24 (Suppl to No 3):106A
- Rougier GW, Apesteeguía S, Gaetano LC (2011) Highly specialized mammalian skulls from the Late Cretaceous of South America. *Nature* 479:98–102
- Rougier GW, Chornogubsky L, Casadio S, Arango NP, Giallombardo A (2009a) Mammals from the Allen Formation, Late Cretaceous, Argentina. *Cret Res* 30:223–238
- Rougier GW, Forasiepi AM, Hill RV, Novacek M (2009b) New mammalian remains from the Late Cretaceous La Colonia Formation, Patagonia, Argentina. *Acta Palaeontol Pol* 54:195–212
- Rougier GW, Leandro G, Drury BR, Colella R, Gomez RO, Arango NP, Calvo J, Porri J, Gonzalez Riga B, Dos Santos D (2010) A review of the Mesozoic mammalian record of South America. In: Calvo J, Porri J, B. Gonzalez Riga B, Dos Santos D (eds) *Paleontología y dinosaurios desde America Latina*. Universidad Nacional de Cuyo, Mendoza, pp 195–214
- Rougier GW, Wible JR, Beck RM, Apesteeguía S (2012) The Miocene mammal *Necrolestes* demonstrates the survival of a Mesozoic nontherian lineage into the late Cenozoic of South America. *Proc Natl Acad Sci USA* 109:20053–20058
- Schultz JA, T Martin (2011) Wear pattern and functional morphology of dryolestoid molars (Mammalia, Cladotheria). *Paläontol Z* 85:269–285
- Sigé B, Sempere T, Butler RF, Marshall LG, Crochet JY (2004) Age and stratigraphic reassessment of the fossil-bearing Laguna Umayo red mudstone unit, SE Peru, from regional stratigraphy, fossil record, and paleomagnetism. *Geobios* 37:771–794.
- Sigogneau-Russell D (2003) Docodonts from the British Mesozoic. *Acta Palaeontol Pol* 48:357–374.
- Simpson GG (1928) A Catalogue of the Mesozoic Mammalia in the Geological Department of the British Museum. Trustees of the British Museum, London, pp 1–215
- Simpson GG (1929) American Mesozoic Mammalia. *Mem Peabody Mus* 3:1–235
- Spradley JP, Pampush JD, Morse PE, Kay RF (2017) Smooth operator: the effects of different 3D mesh retriangulation protocols on the computation of Dirichlet normal energy. *Am J Phys Anthropol* 163:94–109
- Suárez M, Márquez M, De La Cruz R, Navarrete C, Fanning M (2014) Cenomanian–?Early Turonian minimum age of the Chubut Group, Argentina: SHRIMP U-Pb geochronology. *J So Am Earth Sci* 50: 67–74
- Swofford DL (2002) PAUP\* Phylogenetic Analysis Using Parsimony (\*and Other Methods) Version 4. Sinauer Associates, Sunderland
- Wible JR, Rougier GW (2017) Craniomandibular anatomy of the subterranean meridiolestidan *Necrolestes patagonensis* Ameghino, 1891 (Mammalia, Cladotheria) from the early Miocene of Patagonia. *Ann Carnegie Mus* 84:183–252
- Wilf P, NR Cúneo, IH Escapa, D Pol, MO Woodburne (2013) Splendid and seldom isolated: the paleobiogeography of Patagonia. *Annu Rev Earth Planet Sci* 41:561–603
- Wilson GP, Evans AR, Corfe IJ, Smits PD, Fortelius M, Jernvall J (2012) Adaptive radiation of multituberculate mammals before the extinction of dinosaurs. *Nature* 483:457–460
- Wood CB, Dumont ER, Crompton AW (1999) New studies of enamel microstructure in Mesozoic mammals: a review of enamel prisms as a mammalian synapomorphy. *J Mammal Evol* 6:177–213
- Wood CB, Rougier GW (2005) Updating and recoding enamel microstructure in Mesozoic mammals: in search of discrete characters for phylogenetic reconstruction. *J Mammal Evol* 12:433–460
- Woodburne MO, Goin FJ, Bond M, Carlini AA, Gelfo JN, López GM, Inglesias A, Zimicz AN (2014) Paleogene land mammal faunas of South America; a response to global climatic changes and indigenous floral diversity. *J Mammal Evol* 21:1–73
- Vandebroek G (1961) The comparative anatomy of the teeth of lower and non-specialized mammals. *Kon Vlaamse Acad Wetensch Lett Sch Kunsten Belgie* 1:1–215
- Varela JA, Parras A (2013) Análisis tafonómico de una concentración de vertebrados en la Formación La Colonia (Cretácico Tardío), Chubut, Argentina. *Reunión Anual de Comunicaciones de la APA (Córdoba)*. *Ameghiniana* 50:74–75
- Yardeni J (1942) Facts and fancy in dental morphogenesis. *Am J Orthodont Oral Surg* 28:725–735